Research Paper

Exposure to ozone impacted Th1/Th2 imbalance of CD^{4+} T cells and apoptosis of ASMCs underlying asthmatic progression by activating lncRNA PVT1-miR-15a-5p/miR-29c-3p signaling

Yangyang Wei[1,*], Baofen Han[1,*], Wenjuan Dai[1], Shufang Guo[1], Caiping Zhang[1], Lixuan Zhao[2], Yan Gao[2], Yi Jiang[1], Xiaomei Kong[1]

[1]Department of Respiratory and Critical Care Medicine, The First Hospital of Shanxi Medical University, Taiyuan 030001, China
[2]Department of Medicine, Shanxi Medical University, Taiyuan 030001, China
*Equal contribution

Correspondence to: Xiaomei Kong; **email:** kongxiaomei0609@163.com, https://orcid.org/0000-0003-4914-5916
Keywords: asthma, ozone, lncRNA PVT1, miR-15a-5p, miR-29c-3p
Received: January 13, 2020 **Accepted:** September 14, 2020 **Published:** November 20, 2020

ABSTRACT

This investigation attempted to elucidate whether lncRNA PVT1-led miRNA axes participated in aggravating ozone-triggered asthma progression. One hundred and sixty-eight BALB/c mice were evenly divided into saline+air group, ovalbumin air group, saline+ozone group and ovalbumin+ozone group. Correlations were evaluated between PVT1 expression and airway smooth muscle function/inflammatory cytokine release among the mice models. Furthermore, pcDNA3.1-PVT1 and si-PVT1 were, respectively, transfected into CD^{4+}T cells and airway smooth muscle cells (ASMCs), and activities of the cells were observed. Ultimately, a cohort of asthma patients was recruited to estimate the diagnostic performance of PVT1. It was demonstrated that mice of ovalbumin+ozone group were associated with higher PVT1 expression, thicker trachea/airway smooth muscle and smaller ratio of Th1/Th2-like cytokines than mice of ovalbumin air group and saline+ozone group (P<0.05). Moreover, pcDNA3.1-PVT1 significantly brought down Th1/Th2 ratio in CD^{4+} T cells by depressing miR-15a-5p expression and activating PI3K-Akt-mTOR signaling (P<0.05). The PVT1 also facilitated ASMC proliferation by sponging miR-29c-3p and motivating PI3K-Akt-mTOR signaling (P<0.05). Additionally, PVT1 seemed promising in diagnosis of asthma, with favorable sensitivity (i.e. 0.844) and specificity (i.e. 0.978). Conclusively, lncRNA PVT1-miR-15a-5p/miR-29c-3p-PI3K-Akt-mTOR axis was implicated in ozone-induced asthma development by promoting ASMC proliferation and Th1/Th2 imbalance.

INTRODUCTION

Asthma is clinically embodied as repetitive wheeze, dyspnea, chest stress and cough at early morning or in the night, and its global incidence is expected to reach 400 million by 2025 [1]. Even if glucocorticoid-based treatments were efficacious in relieving inflammation of asthma [2], their effects on patients with airflow limitation were not so desirable, which led to skyrocketing mortality [3]. It was widely acknowledged that airway smooth muscle cell (ASMC) and CD^{4+} T cell played crucial roles in airway inflammation and airway remodeling, which exacerbated airflow limitation [4–7]. Specifically, excessive proliferation of ASMCs engendered airway remodeling [8], and promoted airway inflammation by stimulating production of interleukins (e.g. IL-6), chemokines and cell adhesion factors [9]. Biased differentiation of CD^{4+} T cells into Th1-like and Th2-like cells was also responsible for abnormal inflammation in asthma [10]. Taken together, asthma treatment might be improved by restraining ASMC over-proliferation and by preventing Th1/Th2 imbalance.

LncRNAs, a group of ncRNAs with length of > 200 nucleotides, demonstrated huge potential in urging or blocking asthma progression by acting upon miRNAs that mattered in asthmatic inflammation or airway remodeling [11]. For example, knockout of miR-155 was reported to mitigate airway inflammation and airway hyper-responsiveness in ovalbumin (OVA)-sensitized mice [12], so it was probable that lncRNA MALAT1 elevated asthma risk by sponging miR-155 and inhibiting its expression [13]. Of note, expression of lncRNA PVT1 was dramatically lowered in ASMCs that were exposed to anti-asthmatic drugs [14], providing a hint that PVT1 might be associated with ASMC dysfunction underlying asthma etiology. Suppressing PVT1 expression also engendered a marked decrease of IL-6 level, which was reflective of abated inflammation in asthma [15]. Despite hidden linkages between PVT1 and airway remodeling/inflammation, it remained ambiguous whether PVT1 indeed disrupted normal activity of ASMC and CD^{4+} T cell by sponging protective miRNAs in asthma.

In addition, exposure to high-concentration ozone, an alarming phenomenon around the globe (Supplementary Tables 1 and 2), also made human beings vulnerable to asthma [16–18]. In particular, ozone not only facilitated airway smooth muscle contraction by impairing lung function and strengthening airway reactivity [19], but also encouraged abnormal inflammation of T cells through driving neutrophil multiplication [20, 21]. Notably, numerous signaling pathways relevant to immunity were altered under the influence of ozone [22], spanning from NF-κB signaling [23] to miRNA (e.g. miR-149) networks [24]. Nonetheless, few investigations were conducted to figure out if lncRNA-miRNA axes were involved in asthma development triggered by ozone.

Hence, this investigation was carried out to elucidate the association of lncRNA PVT1-led miRNA axes with ozone-induced asthma, which was conducive to clinical prevention and treatment of asthma.

RESULTS

Effect of ozone on airway smooth muscle function of asthma mice models

Bronchial wall and smooth muscle became thicker in OVA+ozone group than in saline+ozone group and OVA+air group (P<0.05) (Figure 1A, 1B). OVA (i.e. OVA+air group) and ozone (i.e. saline+ozone group) treatments also increased airway resistance and decreased lung compliance of mice models, as compared with saline+air group (P<0.05) (Figure 1C, 1D). Furthermore, ozone and OVA seemed interdependent in affecting $LogPC_{100}$ Penh, and OVA+ozone group demonstrated lower $LogPC_{100}$ Penh than saline+air group and OVA+air group (P<0.05) (Figure 1E). Hyaluronan (HA) (Figure 1F), TNF-α (Figure 1G) and IL-13 (Figure 1H) levels also reached a peak in ozone+OVA group, and they were higher in saline+ozone group and OVA+air group than in saline+air group (P<0.05).

Impact of ozone on Th1/Th2 balance of asthma mice models

IL-5, IL-4 and IL-10 levels went higher in OVA+ozone group than in OVA+air group and saline+ozone group (P<0.05) (Figures 1I–1K), indicating that ozone and OVA engendered Th2-biased response more significantly than OVA or ozone alone. On the contrary, Th1-like cytokine levels, including IFN-γ (Figure 1L) and IL-2 (Figure 1M), were restrained in OVA+ozone group in comparison to saline+ozone group and OVA+air group (P<0.05). Moreover, changes of T-bet expression were consistent with that of Th1-like cytokines (Figure 1N), yet expressional variation of GATA3 followed a tendency identical to Th2-like cytokines (Figure 1O).

Association of lncRNA PVT1 expression with airway smooth muscle function and Th1/Th2 balance of asthma mice models

PVT1 expression was significantly elevated in CD^{4+} T cells and ASMCs of OVA+ozone group, as compared with saline+ozone group and OVA+air group (P<0.05) (Figures 2A and 3A). When mice of all subgroups were considered, we found that PVT1 expression in ASMCs was significantly correlated with indicators of airway smooth muscle function, including bronchial wall thickness, smooth muscle thickness, airway resistance, pulmonary compliance, logPC100 Penh, TNF-α level and HA level (Figure 2B). On the other hand, PVT1 expression in CD^{4+} T cells was highly relevant to amount of Th1/Th2-type cytokines (Figure 3B). Intriguingly, the correlations were stronger in mice of OVA+ozone group than in mice of saline+ozone group and OVA+air group (Figures 2C and 3C), suggesting that OVA and ozone might impose additive effects on PVT1 expression in ASMCs and CD^{4+} T cells.

Identification of miRNAs that were involved in PVT1-mediated airway smooth muscle function and Th1/Th2 balance

MiRNAs potentially sponged by PVT1 were predicted with usage of starBase software [25] (Supplementary material), and asthma-relevant miRNAs were measured

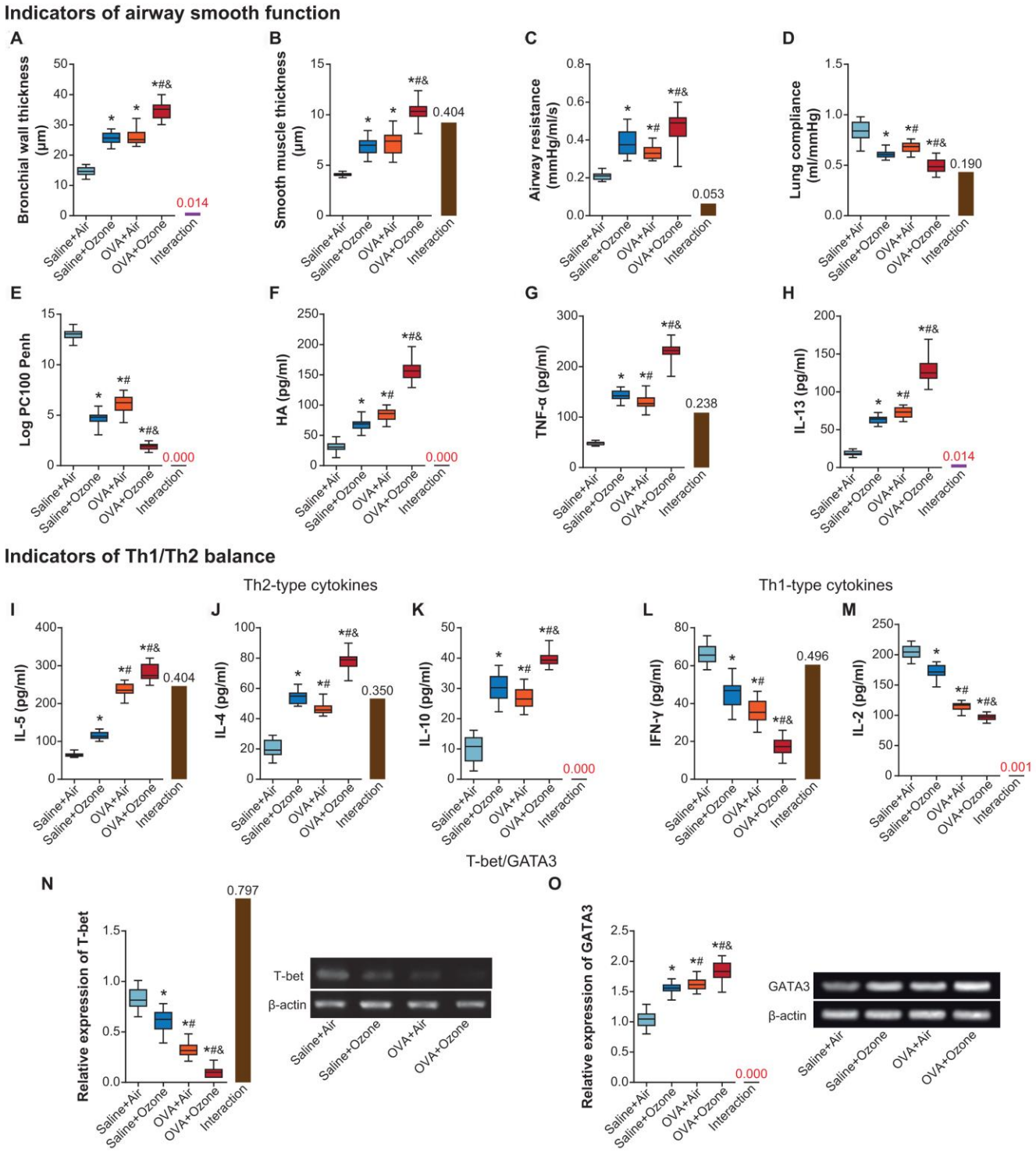

Figure 1. The contribution of ozone exposure to airway smooth function and Th1/Th2 balance of asthmatic mice. (**A**–**E**) The bronchial wall thickness (**A**), smooth muscle thickness (**B**), airway resistance (**C**), lung compliance (**D**) and Log PC100 Penh (**E**) of mice was examined among saline+air, saline+ozone, OVA+air and OVA+ozone groups. *: *P*<0.05 when compared with saline+air group, #: *P*<0.05 when compared with saline+ozone group, &: *P*<0.05 when compared with OVA+air group. (**F**–**H**) Levels of HA (**F**), TNF-α (**G**) and IL-13 (**H**) were determined within mice of saline+air, saline+ozone, OVA+air and OVA+ozone groups. *: *P*<0.05 when compared with saline+air group, #: *P*<0.05 when compared with saline+ozone group, &: *P*<0.05 when compared with OVA+air group. (**I**–**O**) The amounts of IL-5 (**I**), IL-4 (**J**), IL-10 (**K**), IFN-γ (**L**), IL-2 (**M**), T-bet (**N**) and GATA3 (**O**) were determined within mice treated by saline+air, saline+ozone, OVA+air and OVA+ozone. *: *P*<0.05 when compared with saline+air group, #: *P*<0.05 when compared with saline+ozone group, &: *P*<0.05 when compared with OVA+air group.

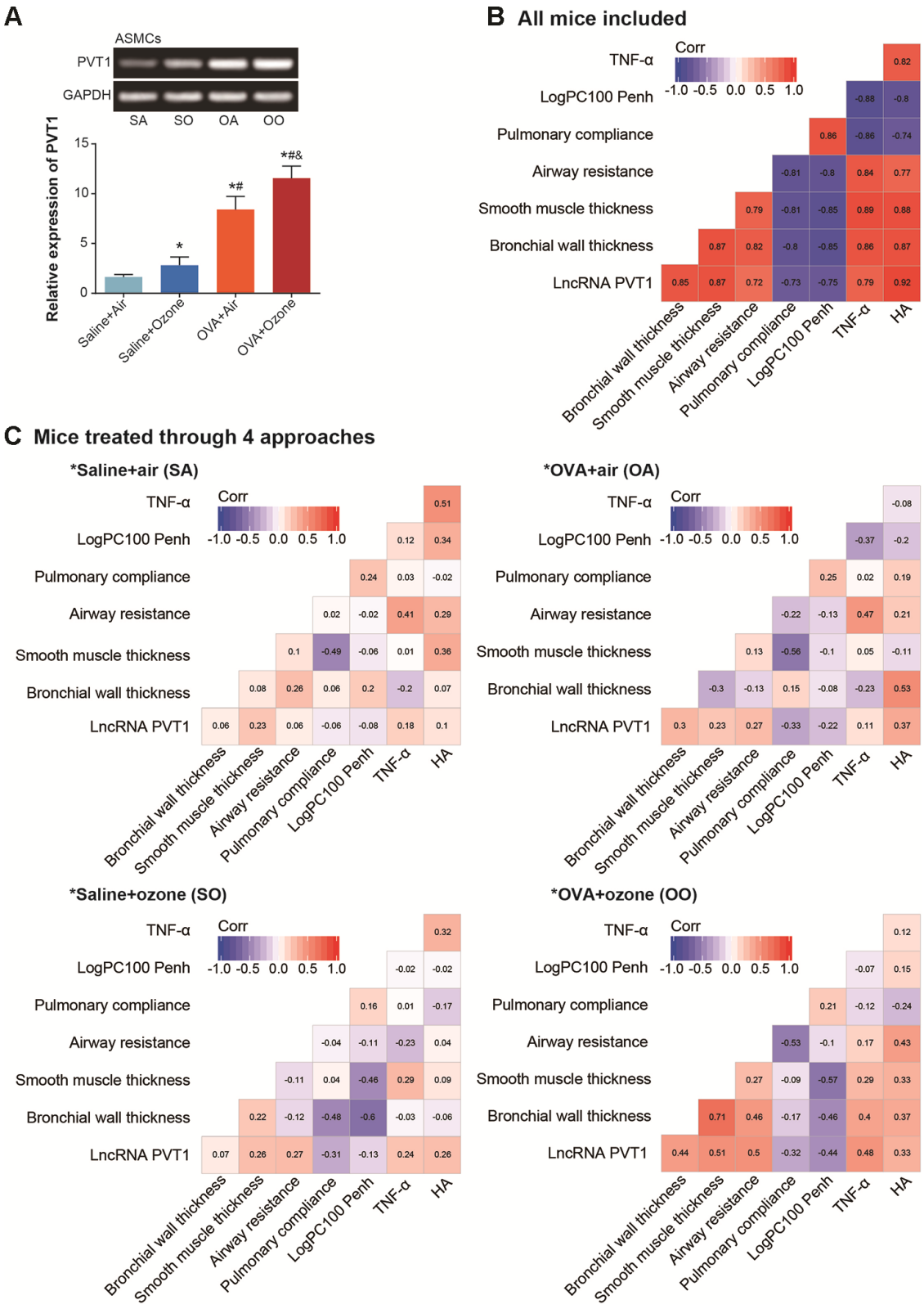

Figure 2. Association of lncRNA PVT1 with airway smooth function of asthmatic mice. (**A**) PVT1 expression was determined within ASMCs that were extracted from mice models of saline+air (SA), saline+ozone (SO), OVA+air (OA) and OVA+ozone (OO) groups. *: *P*<0.05 when compared with SA group, #: *P*<0.05 when compared with saline+ozone group, &: *P*<0.05 when compared with OVA+air group. (**B**, **C**) Correlation matrixes were generated regarding PVT1 expression and airway smooth function in all asthmatic mice (**B**) and in asthmatic mice handled through 4 approaches (**C**).

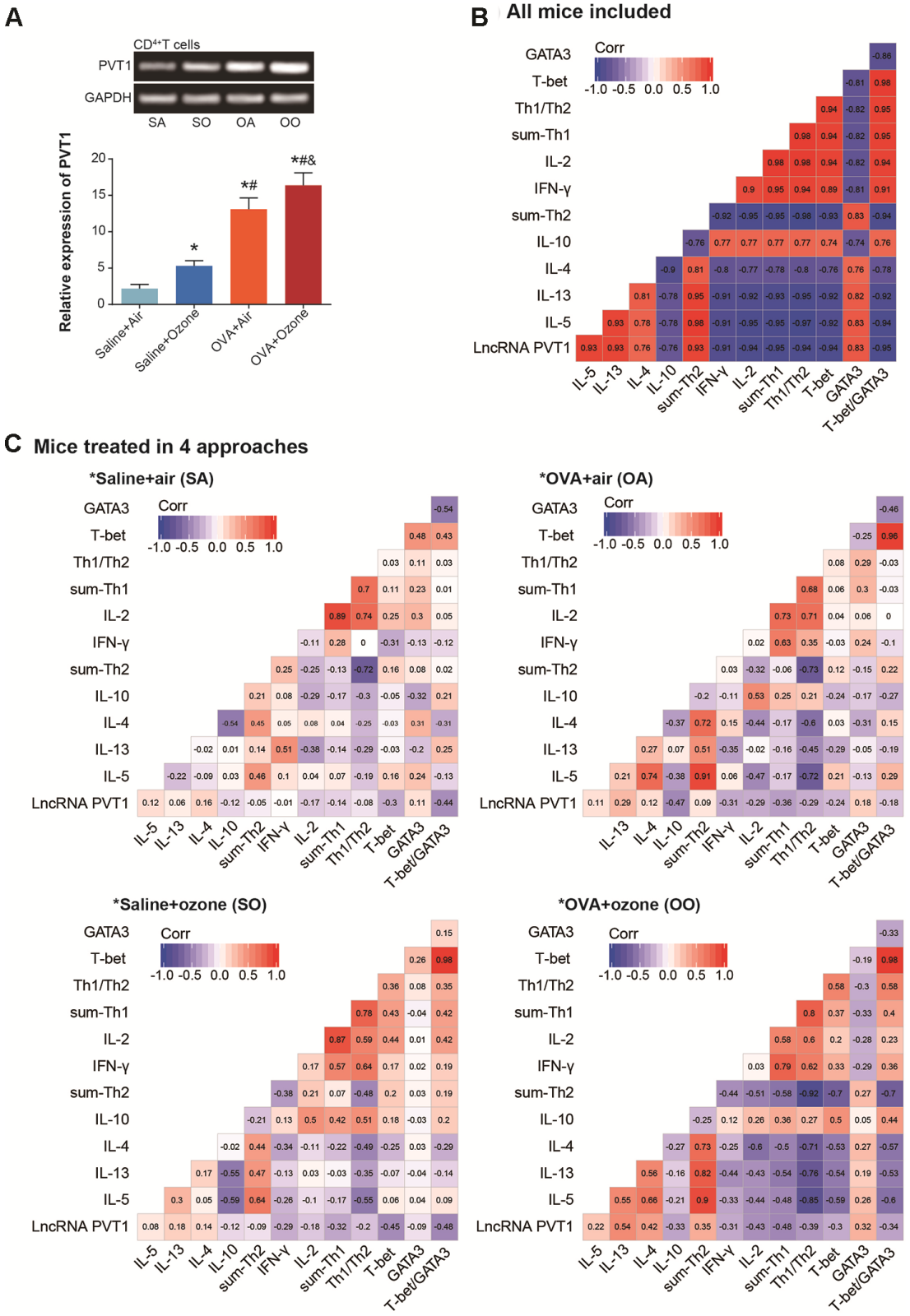

Figure 3. Linkage of lncRNA PVT1 expression with Th1/Th2 balance of asthmatic mice. (**A**) PVT1 expression was monitored within CD^{4+} T cells that were obtained from mice models of saline+air (SA), saline+ozone (SO), OVA+air (OA) and OVA+ozone (OO) groups. *: $P<0.05$ when compared with SA group, #: $P<0.05$ when compared with saline+ozone group, &: $P<0.05$ when compared with OVA+air group. (**B**, **C**) Correlation matrixes were established concerning PVT1 expression and Th1/Th2-specific cytokines in all asthmatic mice (**B**) and in asthmatic mice managed through 4 approaches (**C**).

in CD^{4+} T cells and ASMCs isolated from mice models (Figure 4A and 4B, Supplementary Figure 1). It was demonstrated that miR-15a-5p, miR-140-5p, miR-20b-5p, miR-488-3p and miR-455-5p expressions were significantly down-regulated in CD^{4+} T cells of OVA- and ozone-treated mice (Figure 4A), while miR-29c-3p, miR-143-3p, miR-511-3p, miR-497-5p and miR-488-3p became lowly expressed in ASMCs of OVA/ozone-exposed mice (Figure 4B).

Furthermore, luciferase activity of CD^{4+} T cells in the miR-15a-5p/miR-20b-5p mimic+pGL3-PVT1-Wt group was decreased in comparison to miR-NC+pGL3-PVT1-Wt group and miR-15a-5p/miR-20b-5p mimic+pGL3-PVT1-Mut group (P<0.05) (Figure 4C). And miR-15a-5p/miR-20b-5p expression in CD^{4+} T cells was up-regulated by si-PVT1 and down-regulated by pcDNA3.1-PVT1 (P<0.05), suggesting that miR-15a-5p and miR-20b-5p in CD^{4+} T cells were suppressed after being sponged by PVT1. Concerning ASMCs, their luciferase activity was attenuated in the miR-29c-3p/miR-143-3p/miR-511-3p mimic+pGL3-PVT1-Wt group, when compared with miR-NC+pGL3-PVT1-Wt group and miR-29c-3p/miR-143-3p/miR-511-3p mimic+pGL3-PVT1-Mut group (P<0.05) (Figure 4D). And miR-29c-3p and miR-143-3p expressions were lessened by pcDNA3.1-PVT1 and yet increased by silencing of PVT1 (P<0.05), implying that PVT1 possibly sponged miR-29c-3p/miR-143-3p and inhibited their expression.

What's more, PI3K-Akt signaling and mTOR signaling were KEGG pathways enriched by genes targeted by significant miRNAs in CD^{4+} T cells and ASMCs (Figure 5), which was draw from miRPath software [26]. Interestingly, the PI3K-Akt-mTOR signaling counted much in lung inflammation and airway remodeling of asthma [27–32], and they were involved in propelling ozone-stimulated oxidative stress [33, 34]. It was thus speculated that PVT1-miRNA axis might participate in ozone-induced asthma development by activating PI3K/Akt/mTOR signaling.

PVT1 sponged miR-29c-3p to facilitate proliferation and depress apoptosis of ASMCs

PVT1 expression in ASMC was elevated dramatically after transfection of pcDNA3.1-PVT1, yet its expression revealed a drop when si-PVT1 was transfected (P<0.05) (Figure 6A). Moreover, pcDNA3.1-PVT1 strengthened viability and proliferation, yet hindered apoptosis of ASMCs (P<0.05) (Figure 6B–6D). By contrast, viability and proliferation of ASMCs were weakened, and ASMC apoptosis was accelerated by si-PVT1 (P<0.05). Furthermore, bax/caspase-3 expressions were down-regulated, and bcl-2 expression was up-regulated in cases of pcDNA3.1-PVT1 transfection (P<0.05), whereas si-PVT1 group exhibited higher bax/caspase-3 expressions and lower bcl-2 expression than si-NC group (P<0.05) (Figure 6E). It was noteworthy that viability and proliferation of ASMCs were impaired in the pcDNA3.1-PVT1+miR-29c-3p mimic group in comparison to pcDNA3.1-PVT1 group (P<0.05) (Figure 6F and 6G), yet ASMC apoptosis was boosted in the pcDNA3.1-PVT1+miR-29c-3p mimic group as relative to pcDNA3.1-PVT1 group (P<0.05) (Figure 6H). Expressions of caspase-3 and bax were also raised, along with decreased expression of bcl-2, in pcDNA3.1-PVT1+miR-29c-3p mimic group, when compared with pcDNA3.1-PVT1 group (P<0.05) (Figure 6I).

PI3K/AKT signaling reversed inhibition of miR-29c-3p on ASMC viability, proliferation and apoptosis

Expressions of p-PI3K, p-AKT and p-mTOR in ASMCs were heightened by pcDNA3.1-PVT1 or miR-29c-3p inhibitor (P<0.05), and they were suppressed by si-PVT1 and miR-29c-3p mimic (P<0.05) (Figure 7A). However, IGF-1 (i.e. activator of PI3K/AKT signaling) and LY294002 (i.e. inhibitor of PI3K/AKT signaling) treatments failed to alter PVT1 and miR-29c-3p expressions in ASMCs (P>0.05) (Figure 7B). In addition, proliferation and viability of ASMCs were significantly motivated in the miR-29c-3p mimic+IGF-1 group as compared with miR-29c-3p mimic group (P<0.05) (Figure 7C and 7D), and ASMCs in the miR-29c-3p mimic+IGF-1 group were less prone to apoptosis than ASMCs in the miR-29c-3p mimic group (P<0.05) (Figure 7E and 7F).

PVT1/miR-15a-5p axis promoted Th1/Th2 imbalance of CD^{4+}T cells by activation of PI3K-AKT signaling

PVT1 expression was significantly increased in CD^{4+} T cells transfected by pcDNA3.1-PVT1 (P<0.05), and was decreased by transfection of si-PVT1 (P<0.05) (Figure 8A). MiR-15a-5p expression in CD^{4+} T cells was enhanced by miR-15a-5p mimic (P<0.05), and was diminished by miR-15a-5p inhibitor (P<0.05) (Figure 8A). Moreover, pcDNA3.1-PVT1 and miR-15a-5p inhibitor were found to activate p-PI3K, p-AKT and p-mTOR in CD^{4+} T cells (P<0.05), which were deactivated by si-PVT1 and miR-15a-5p mimic (P<0.05) (Figure 8B). Nevertheless, expressions of PVT1 and miR-15a-5p in CD^{4+} T cells were almost unchanged by IGF-1 and LY29400, when compared with untreated CD^{4+} T cells (P>0.05) (Figure 8C). Furthermore, CD^{4+} T cells of miR-15a-5p mimic+IGF-1 group engendered lower protein levels of IFN-γ, IL-2 and T-bet and higher protein levels of IL-4, IL-10 and GATA3 than CD^{4+} T cells of miR-15a-5p mimic group (P<0.05) (Figure 8D).

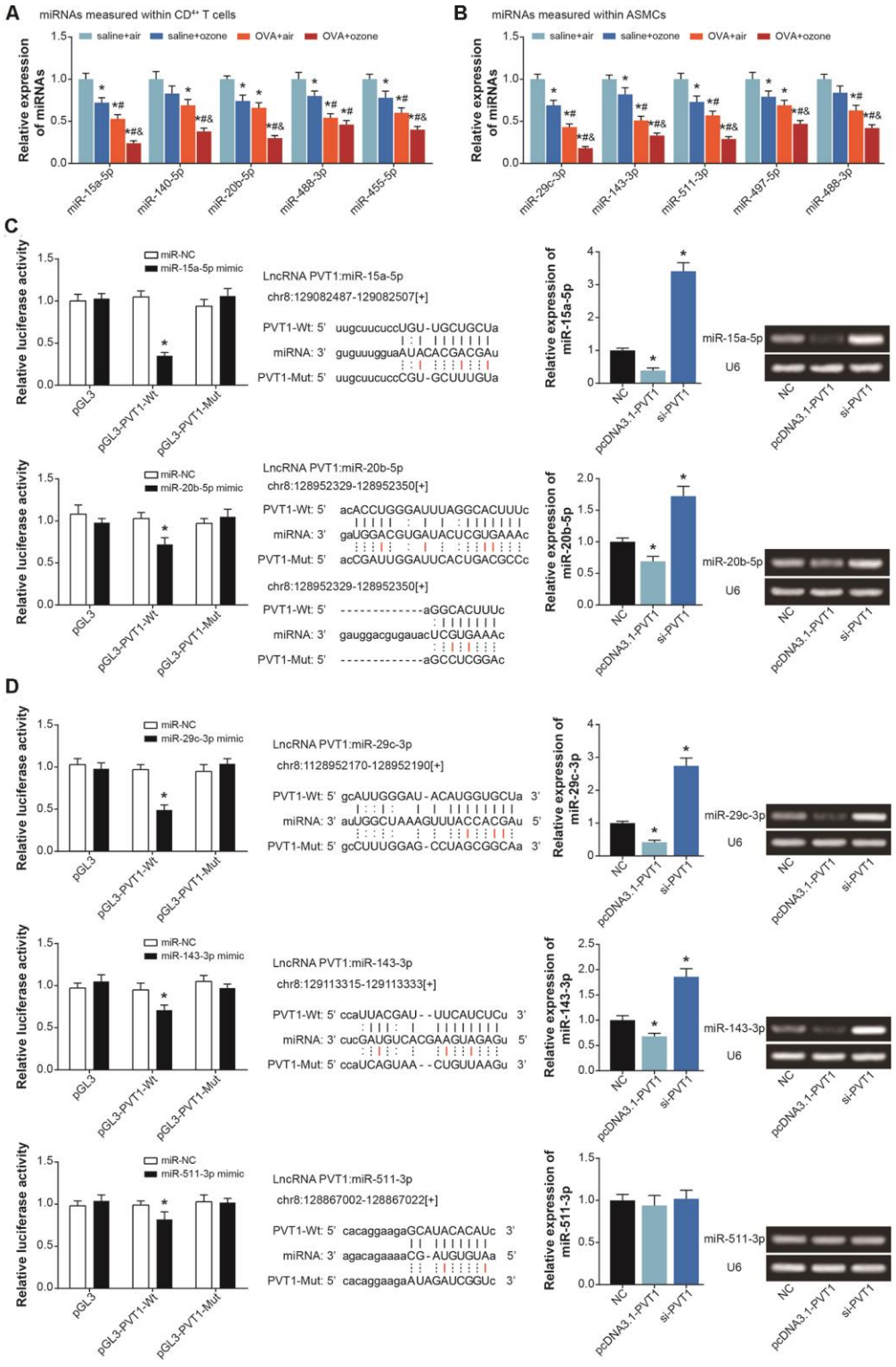

Figure 4. MiRNAs potentially sponged by lncRNA PVT1 within ASMCs and CD^{4+} T cells. (**A**) MiR-15a-5p, miR-140-5p, miR-20b-5p, miR-488-3p and miR-455-5p were differentially expressed within CD^{4+} T cells of saline+air, saline+ozone, OVA+air and OVA+ozone groups. *: *P*<0.05 when compared with SA group, #: *P*<0.05 when compared with saline+ozone group, &: *P*<0.05 when compared with OVA+air group. (**B**) Expressions of miR-29c-3p, miR-143-3p, miR-511-3p, miR-497-5p and miR-488-3p were evaluated within ASMCs of mice models among saline+air, saline+ozone, OVA+air and OVA+ozone groups. *: *P*<0.05 when compared with SA group, #: *P*<0.05 when compared with saline+ozone group, &: *P*<0.05 when compared with OVA+air group. (**C**) MiR-15a-5p and miR-20b-5p were sponged and regulated by lncRNA PVT1 in CD^{4+} T cells. (**D**) MiR-29c-3p, miR-143-3p and miR-511-3p were subjected to sponged modulation by lncRNA PVT1 in ASMCs.

A

KEGG pathway	p-value	#genes	#miRNAs
Pathways in cancer	0.001092	112	8
PI3K-Akt signaling pathway	**3.53E-05**	**106**	**9**
Focal adhesion	4.19E-05	72	9
Regulation of actin cytoskeleton	0.039702	60	9
Proteoglycans in cancer	0.025436	52	9
Signaling pathways regulating pluripotency of stem cells	2.25E-05	51	8
cGMP-PKG signaling pathway	0.006125	51	8
Hippo signaling pathway	2.92E-06	49	8
Insulin signaling pathway	0.006125	46	9
AMPK signaling pathway	0.004922	42	8
Wnt signaling pathway	0.025436	42	8
Ubiquitin mediated proteolysis	0.039702	40	8
Choline metabolism in cancer	0.000774	39	9
FoxO signaling pathway	0.015829	39	8
Adrenergic signaling in cardiomyocytes	0.033791	39	8

B

KEGG pathway	p-value	#genes	#miRNAs
Pathways in cancer	2.99E-05	79	5
PI3K-Akt signaling pathway	**0.022621**	**60**	**6**
Rap1 signaling pathway	0.016628	45	5
Proteoglycans in cancer	4.98E-05	44	6
Focal adhesion	0.009109	44	6
Regulation of actin cytoskeleton	0.022621	43	6
Signaling pathways regulating pluripotency of stem cells	4.48E-08	41	5
Hippo signaling pathway	4.98E-05	38	5
cGMP-PKG signaling pathway	0.03251	33	5
Wnt signaling pathway	0.002281	32	5
Ubiquitin mediated proteolysis	0.003224	32	5
Insulin signaling pathway	0.013691	32	6
Prostate cancer	4.81E-05	28	5
Neurotrophin signaling pathway	0.018102	28	4
Dopaminergic synapse	0.032642	28	5

Figure 5. The enrichment pathways of significantly-expressed miRNAs in CD^{4+} T cells (**A**) and ASMCs (**B**) were drawn based on miRPath software.

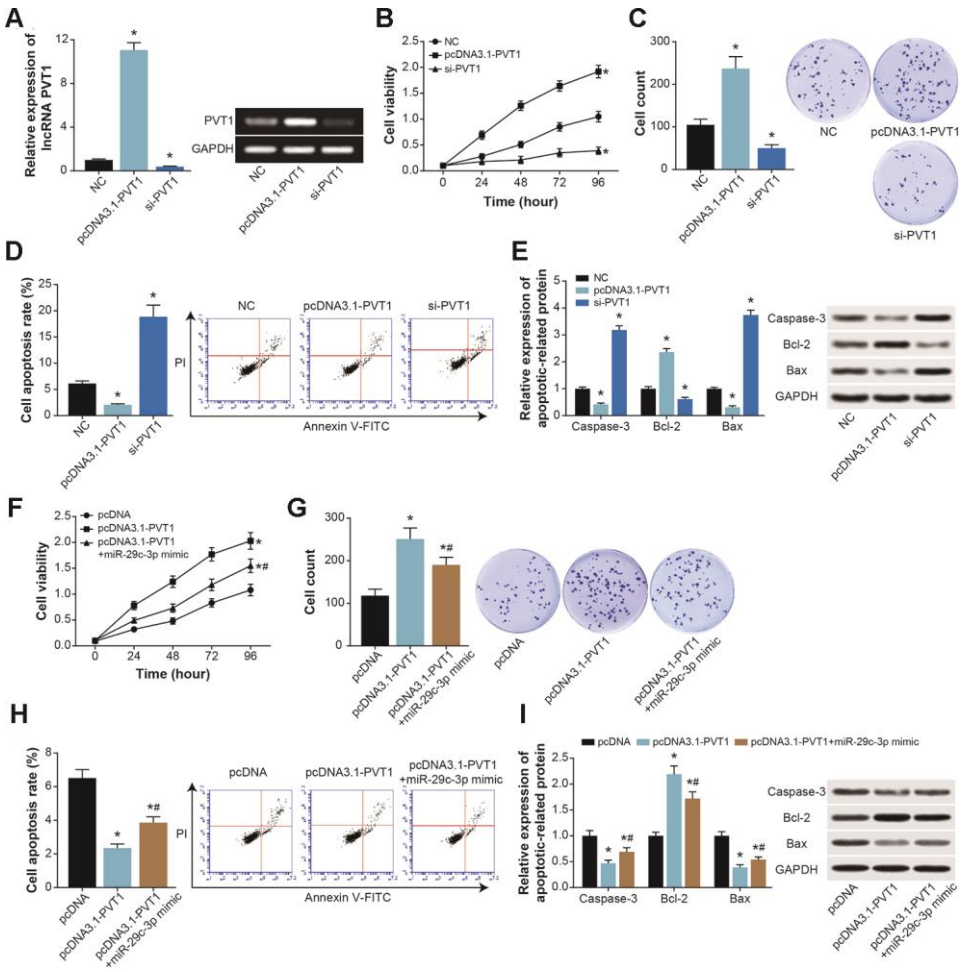

Figure 6. The effects of PVT1 and miR-29c-3p on proliferation and apoptosis of ASMCs. (**A**) PVT1 expression in ASMCs was determined after transfection of pcDNA-PVT1 and si-PVT1. *: *P*<0.05 when compared with NC group. (**B**–**D**) The viability (**B**), proliferation (**C**) and apoptosis (**D**) of ASMCs were compared after transfections of pcDNA-PVT1 and si-PVT1. *: *P*<0.05 when compared with NC group. (**E**) The expressions of apoptotic proteins within ASMCs were compared under treatments of pcDNA-PVT1and si-PVT1. *: *P*<0.05 when compared with NC group. (**F**–**H**) The viability (**F**), proliferation (**G**) and apoptosis (**H**) of ASMCs were evaluated among pcDNA3.1, pcDNA3.1-PVT1 and pcDNA3.1-PVT1+miR-29c-3p mimic groups. *: *P*<0.05 when compared with pcDNA3.1 group, #: *P*<0.05 when compared with pcDNA3.1-PVT1 group. (**I**) Expressions of apoptins were measured within ASMCs of pcDNA3.1, pcDNA3.1-PVT1 and pcDNA3.1-PVT1+miR-29c-3p mimic groups. *: *P*<0.05 when compared with pcDNA3.1 group, #: *P*<0.05 when compared with pcDNA3.1-PVT1 group.

Diagnostic performance of PVT1 in asthma

Higher serum levels of TNF-α, IL-13, IL-4, IL-10, hs-CRP and FeNO were determined in asthma patients than in healthy volunteers (P<0.05) (Supplementary Table 3). The cytokine levels also demonstrated an upward trend in patients with acute asthma when compared with patients in the remission stage of asthma (P<0.05). Conversely, asthma patients were associated with smaller FEV1 and lower FEV1/FVC ratio than healthy controls (P<0.05), and both FEV1 and FEV1/FVC ratio were lessened in patients with acute asthma as compared with asthma patients in remission stage (P<0.05). Serum level of PVT1 also went up significantly in asthma patients when compared with healthy controls (P<0.05), and patients with acute asthma revealed higher PVT1 expression than asthma patients in remission stage (P<0.05) (Supplementary Figure 2A). It seemed that PVT1 was promising in diagnosis of asthma (AUC=0.909) (Supplementary Table 4, Supplementary Figure 2B) and in differentiating patients with acute asthma from asthma patients in remission stage (AUC=0.705) (Supplementary Table 4, Supplementary Figure 2C).

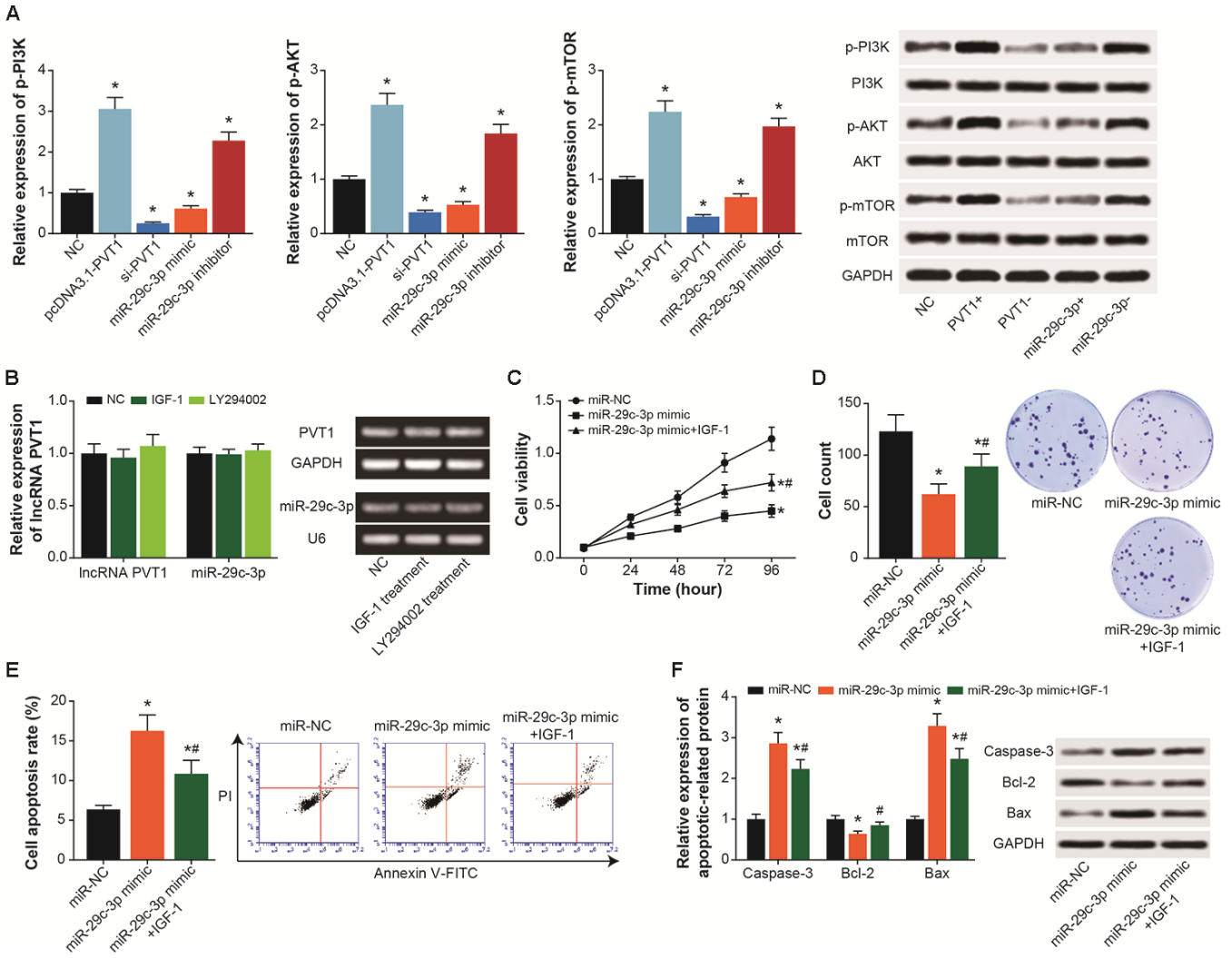

Figure 7. PI3K/AKT/mTOR signaling mediated the impact of PVT1/miR-29c-3p axis on ASMC activity. (**A**) Expressions of p-PI3K, PI3K, p-AKT, AKT, p-mTOR and mTOR were determined within ASMCs that were treated by none, pcDNA3.1-PVT1, si-PVT1, miR-29c-3p mimic and miR-29c-3p inhibitor. *: P<0.05 when compared with NC group. (**B**) Expressions of PVT1 and miR-29c-3p were assessed in ASMCs managed by IGF-1 and LY294002. *: P<0.05 when compared with NC group. (**C**–**E**) Viability (**C**), proliferation (**D**) and apoptosis (**E**) of ASMC were appraised among miR-NC, miR-29c-3p mimic and miR-29c-3p mimic+IGF-1 groups. *: P<0.05 when compared with miR-NC group, #: P<0.05 when compared with miR-29c-3p mimic group. (**F**) Expressions of apoptins were measured within ASMCs of miR-NC, miR-29c-3p mimic and miR-29c-3p mimic+IGF-1 groups. *: P<0.05 when compared with miR-NC group, #: P<0.05 when compared with miR-29c-3p mimic group.

DISCUSSION

Here we attempted to uncover whether lncRNA PVT1-miRNA axis was implicated in the pathogenesis of ozone-induced asthma. Firstly, mice models of asthma were established [35], and it was intriguing to notice that acute exposure to ozone aggravated asthma symptoms in OVA-exposed mice models [36] (Figure 1). Specifically, airway wall and airway smooth muscle were thickened (Figure 1A and 1B), along with intensified airway stenosis, in ozone-exposed asthmatic mice (Figure 1C and 1D), suggesting that ozone drove airway remodeling and suppressed pulmonary compliance of asthmatic mice. Changes of log100 Penh value (Figure 1E), determined by means of pneumotachograph of whole-body plethysmography [37], reflected that airway responsiveness of asthmatic mice was reduced after exposure to ozone, and the noticeable increase in levels of TNF-α and HA (Figure 1F and 1G) suggested that ASMC proliferation in OVA-exposed mice was promoted by ozone [38–41]. In addition to airway function controlled by ASMC, Th1/Th2 balance manipulated by CD^{4+} T cells was also aggravated by OVA exposure and ozone [10, 42, 43], detailed as that ozone increased Th2/Th1 ratio (Figure 1I-1M) and decreased T-bet/GATA3 ratio (Figure 1N and 1O) in OVA-exposed mice.

There have been evidence that ozone triggered asthma onset by inducing airway responsiveness and airway inflammation [44–46]. The proponents held that oxygen free radicals generated by ozone attacked intra-membranous polyunsaturated fatty acid and triggered oxidative damage in organisms [47–49], which finally worsened inflammation in airway [50, 51]. However, a contradiction existed that prevalence of asthma was disproportionate to worldwide concentration of ozone (https://www.stateofglobalair.org/data/#/air/map) (Supplementary Tables 1 and 2) [52]. We speculated that distinctions in detecting instrument, operation step and measurement standard might blur the actual impact of ozone on asthma onset. Other contributors to asthma, such as family history and abrupt climate change, could also confuse the internal association of ozone with asthma development. Of note, PVT1, which contained a genomic region indicative of high cancer risk [53, 54], was conjectured to involve in ozone-caused asthma progression, allowing for that PVT1 expression was strongly correlated with ASMC function and Th1/Th2 balance of ozone-treated asthma mice models (Figures 2, 3). This might be ascribed to the strength of PVT1 in promoting ASMC multiplication and in boosting secretion of Th2-type cytokines as opposed to Th1-type cytokines by CD^{4+} T cells.

Founded on the ceRNA theory, we suspected that PVT1 probably urged asthma progression by sponging miR-15a-5p and miR-29c-3p, two protective miRNAs in asthma [55]. The miR-15a-5p was documented to hinder production of inflammatory chemokines (e.g.

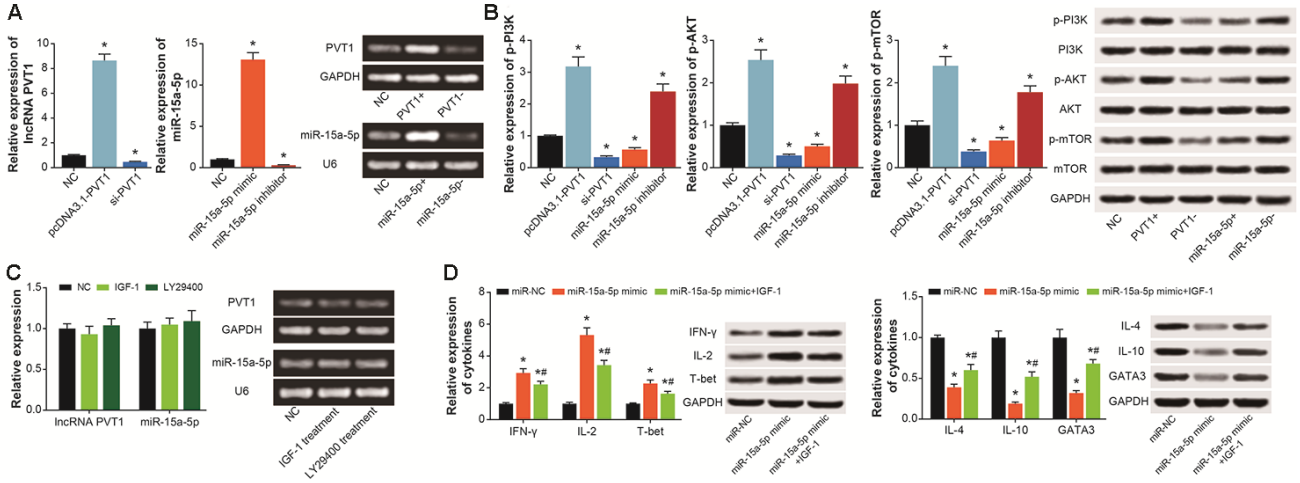

Figure 8. PI3K/AKT/mTOR signaling was implicated in the contribution of PVT1/miR-15a-5p axis to Th1/Th2 balance in CD^{4+} T cells. (**A**) PVT1 expression was determined after transfection of pcDNA3.1-PVT1 and si-PVT1, and miR-15a-5p level was compared in CD^{4+} T cells transfected by miR-15a-5p mimic and inhibitor. *: *P*<0.05 when compared with miR-NC group. (**B**) The p-PI3K, PI3K, p-AKT, AKT, p-mTOR and mTOR expressions in CD^{4+} T cells were figured out among NC, pcDNA3.1-PVT1, si-PVT1, miR-15a-5p mimic and miR-15a-5p inhibitor groups. *: *P*<0.05 when compared with NC group. (**C**) PVT1 and miR-15a-5p expressions were obtained from CD^{4+} T managed by IGF-1 and LY294002. *: *P*<0.05 when compared with NC group. (**D**) The levels of cytokines relevant to Th1/Th2 imbalance were determined within CD^{4+} T cells among miR-NC, miR-15a-5p mimic and miR-15a-5p mimic+IGF-1 groups. *: *P*<0.05 when compared with miR-NC group, #: *P*<0.05 when compared with miR-15a-5p mimic group.

IL-10) [56], and to prevent onset of T cell-relevant diseases [57]. Here PVT1 was speculated to promote Th2-orineted inflammation in CD^{4+} T cells by resisting function of miR-15a-5p (Figure 4C, Figure 8D), which was a highlight of this study. With regard to miR-29c-3p, which was down-regulated in asthma children [58], we found it effective in reversing the contribution of PVT1 to ASMC proliferation and viability (Figure 6F–6I). Despite difference in cell type, miR-29c-3p was capable of holding up proliferation, invasion and metastasis of tumor cells [59, 60], including lung cancer, hepatic carcinoma, gastric cancer, glioma and leukemia [61–63], And this might explain why miR-29c-3p prevented ASMC abnormality in asthma from the molecular side.

In addition, PI3K/Akt/mTOR signaling was a widely-recognized driver of airway inflammation and airway remodeling underlying asthma etiology. For instance, PI3K was able to reinforce inflammation response mediated by eosinophilic granulocyte, T cell, mastocyte and neutrophil, which stayed core to asthma onset [64]. Th2-centric inflammation response was also promoted by PI3K [65], and Akt activation tended to guide differentiation of Th cells into Th2-like CD^{4+} T cells [66]. Furthermore, PI3K-dependent P70S6K activation was implicated in controlling mitogen-stimulated response of ASMC [67], and PI3K/Akt/mTOR signaling was capable of worsening airway remodeling by stimulating ASMC proliferation [68–72]. Our study newly introduced that PI3K/Akt/mTOR signaling not merely diminished the effect of miR-15a-5p on Th1/Th2 balance in CD^{4+} T cells (Figure 8D), but also undermined the impact of miR-29c-3p on ASMC proliferation (Figure 7C–7F), which expanded knowledge about asthma pathogenesis.

CONCLUSIONS

In conclusion, this investigation tentatively verified that ozone exacerbated asthma development by activating PVT1-miR-15a-5p/miR-29c-3p signaling, which motivated Th1/Th2 imbalance of CD^{4+} T cells and urged excessive proliferation of ASMCs (Figure 9). Nonetheless, although cell models and animal models were established, clinical evidence was insufficient to support this hypothesis, which necessitated more convincing evidence. Secondly, genes that encoded oxidative/non-oxidative enzymes were not detected, so impacts of ozone and OVA on in-vivo oxidative stress could not be verified. Last but not the least, ozone level applied here was above the concentration of natural exposure and also exceeded the concentration which induced asthma onset (i.e. 0.06 ppm) [73]. It might be better if later researches were designed to tally with practical settings.

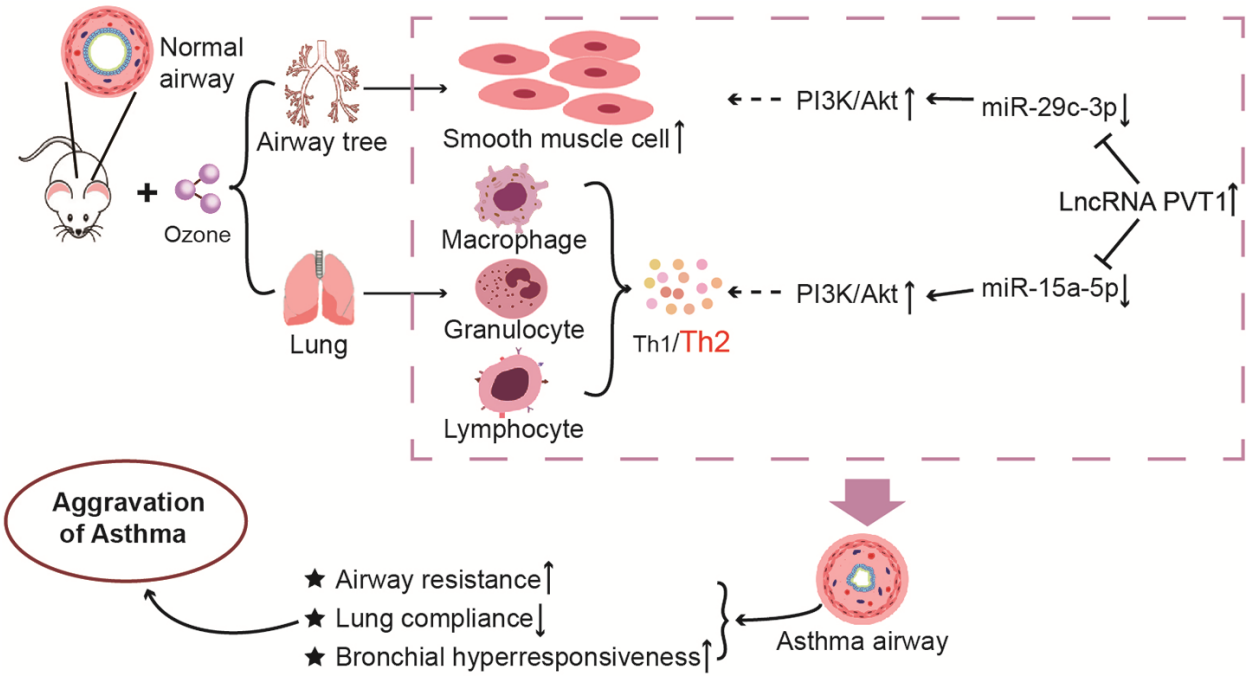

Figure 9. The mechanism diagram about impacts of lncRNA PVT1–centered miRNA networks and ozone on asthmatic progression. It was revealed that exposure to ozone impacted Th1/Th2 imbalance of CD^{4+} T cells by regulating lncRNA PVT1-miR-15a-5p-PI3K/AKT/mTOR axis and apoptosis of ASMCs through modifying lncRNA PVT1-miR-29c-3p- PI3K/AKT/mTOR axis.

MATERIALS AND METHODS

Establishment of mice models with acute asthma

A total of 168 female BALB/C mice, aged 8-10 weeks old and weighing around 20 g, were purchased from Shanghai Laboratory Animal Center (Shanghai, China). The mice, exposed under a 12h/12h light/dark cycle, were housed in individually ventilated cages that were controlled at a 24° C and in 60% humidity. We divided the mice into saline+air group (n=42), OVA+air group (n=42), saline+ozone (n=42) group and OVA+ozone (n=42) group, and their treatments were particularized in Supplementary Figure 3.

Assessment of airway resistance and pulmonary compliance in asthma mice models

After being anesthetized by 80 mg/kg pentobarbital for 10 min, trachea of mice models was separated by cutting cervical region and peeling upper airway. The trachea was cut between the 2nd and the 3rd cricoid cartilage, and a cannula (diameter: 0.9 mm) was inserted into the airway until a depth of 3-4 mm. Then a knot was tied to fix the 4th and the 5th trachea cartilage ring, and cannula was connected to animal ventilator (model: SAR-830, CWE corporation, USA). Airway resistance (R) and pulmonary compliance of mice models were automatically calculated by MF Lab software (version 3.01).

Evaluation of bronchial reactivity and airway hyper-responsiveness (AHR) in asthma mice models

Bronchial reactivity of mice models was monitored using non-invasive whole-body plethysmograph (model: FinePointe™NAM, Bucxo, USA). Basic enhanced pause (Penh) value and Penh values under treatments of 0, 1.56, 3.12, 6.25, 12.5, 25 and 50g/L methacholine (MCH) were detected [74], and airway reactivity was calculated according to the formula of $\frac{\text{average Penh value within 7 min}}{\text{basal } Penh\, value} \times 100\%$. AHR (i.e. Log PC_{100}) was equivalent to the logarithm of MCH concentration that mice required to achieve 2 folds of their basal airway responsiveness.

Measurement of bronchoalveolar cytokines in asthma mice models

A polyethylene catheter (diameter: 1.0 mm) was inserted into the slot which was cut between the 2nd and the 3rd cartilaginous rings of mice models. Then icy PBS was injected into lung of mice models with a syringe (model: 1 ml), and 80% of the lavage fluid was recycled. After centrifugation at 7500×g for 5 min, IL-5, IL-13, TNF-α, HA, IFN-γ, IL-2, IL-4 and IL-10 levels in the supernatant were determined with ELISA kits (R&D Systems, USA).

Appraisal of bronchial wall/smooth muscle thickness in asthma mice models

Lung hilum cut from mice models was immersed within 4% paraformaldehyde, and 6 h later they were immersed in 70% ethanol and embedded by paraffin. Slices stained by hematoxylin-eosin (HE) were observed under 200× light microscope, and bronchial walls with complete structure were selected. Circumferential diameter of bronchial basement membrane (Pbm), total area of bronchial wall (Wat) and area of bronchial smooth muscle (Wam) were gauged aided by IPP 6.0 image analysis software. Wat/Pbm ratio and Wam/Pbm ratio were, respectively, indicative of bronchial wall thicknesses and smooth muscle thicknesses.

Isolation of CD^{4+} T cells and ASMCs from asthma mice models

Isolation of CD^{4+} T cells from spleen of mice models

After centrifugation at the spend of 2000 r/min, monocytes were re-suspended within 5 ml RPMI1640 medium which contained 10% FCS (Gibco, USA). Monocytes adjusted to the concentration of 1×10^8/ml were incubated with 1 ml rat anti-mouse CD4 antibody (eBioscience, USA) for 15 min at room temperature. Then cell suspension that flew through separation column (R&D Systems, USA) was collected, until liquid effluent became clear.

Extraction of ASMCs from trachea of mice models

Tracheal of mice models was separated, and their bronchus was vertically dissected and cut into tissue blocks sized as 1 mm^3. The cells were then cultivated in 5% CO_2 at 37° C, until digestion by 0.25% trypsin on the 10th day. ASMCs were confirmed by performing α-actin immune-cytochemical staining.

Cell transfection

With assistance of Lipofectamine® RNAiMAX transfection kit (Thermo Fisher Scientific, USA), si-PVT1 (Genepharma, China), si-NC, pcDNA3.1-PVT1 (Genepharma, China), miR-15a-5p mimic and miR-15a-5p inhibitor (Ribobio, China) were, respectively, transfected into CD^{4+} T cells. On the other hand, si-PVT1, pcDNA3.1-PVT1, miR-29c-3p mimic and miR-29c-3p inhibitor (Genepharma, China) were transfected into ASMCs, respectively. ASMCs and CD^{4+} T cells were cultivated within Opti-MEM® reduced serum medium (Thermo Fisher Scientific, USA), until they grew to > 70% confluency.

Cell treatment

CD^{4+} T cells and ASMCs were treated by insulin-like growth factor (IGF-1, Peprotech, USA) at the final concentration of 1 μmol/L or LY294002 (Selleck, USA) at the final concentration of 50 μmol/L.

Evaluation of ASMC activity

CCK-8 assay

ASMCs inoculated at the concentration of 1×10^4/ml were cultivated until they became adherent to the plate wall. Then ASMCs of each well were incubated by 10 μl CCK 8 reagent (DOJINDO, Japan) for 4 h. Absorbance (A) of ASMCs was measured on the enzyme-linked immunosorbent assay system (model: ElX800, BIO-TECH, USA) at the wavelength of 450 nm.

Colony formation assay

ASMCs at the density of 4×10^3/well were cultured in 6-well plates for 9 days, and then they were fixed by 4% paraformaldehyde for 15 min and dyed by 0.1 % crystal violet for 20 min. Photographs were taken after air-dry of ASMCs.

Cell apoptosis assay

When ASMCs (concentration: 1×10^5/well) grew to cover 70% of cell plate, they were mixed by 10 μl Annexin V-FITC (Sigma, USA) and 5 μl propidium iodide (PI) (Sigma, USA). After 15-min culture in the darkness, percentage of apoptotic ASMCs was assessed on flow cytometer (model: FACSAria, BD, USA).

Collection of blood samples from asthma patients

One hundred and forty-seven patients with asthma were recruited from The First Hospital of Shanxi Medical University. The asthma patients were all in accordance with diagnostic criteria formulated by Chinese Society of Respiratory Medicine [75], including 85 patients at the acute stage of asthma and 62 asthma patients in remission stage. Asthma patients in remission stage should not show any acute asthma symptoms in the past $\geq$ 1 month, and patients with acute asthma were given glucocorticoids-/bronchodilators-based treatments. Meanwhile, 46 healthy volunteers without any history of allergic diseases were incorporated, and they should not suffer from any infectious diseases for the past 2 months. All the participants have signed informed consents, and this program was approved by The First Hospital of Shanxi Medical University and the ethics committee of The First Hospital of Shanxi Medical University. Around 4 ml venous blood was taken from each subject, which was reserved at -80° C for PVT1 detection with RT-PCR.

Western blotting

Concentration of total proteins, extracted from tissues and cells with RIPA buffer, was measured with BCA kit (Beyotime, China). After undergoing 10% sodium dodecyl sulfate-polyacrylamide gel electrophoresis (SDS-PAGE), protein samples were electrically transferred onto polyvinylidene fluoride (PVDF) membrane for 3 h. Afterwards, the samples were blocked by 5% skim milk for 1 h, followed by incubation with primary antibodies (rabbit anti-mouse, Abcam, USA) against caspase-3 (1: 500, Catalog No.: ab13847, Abcam), Bcl-2 (1: 2000, Catalog No.: ab196495, Abcam), Bax (1: 3000, Catalog No.: ab32503, Abcam), p-PI3K (1:1000, Catalog No.:17366, Cell Signaling Technology), PI3K (1:1000, Catalog No.:4292, Cell Signaling Technology), p-AKT (1:2000, Catalog No.: 4060, Cell Signaling Technology), AKT (1:1000, Catalog No.:4691, Cell Signaling Technology), p-mTOR (1:1000, Catalog No.:5536, Cell Signaling Technology), mTOR (1:1000, Catalog No.:2972, Cell Signaling Technology), IFN-γ (1: 3000, Catalog No.: ab171081, Abcam), IL-2 (1:500, Catalog No.: ab180780, Abcam), T-bet (1:1000, Catalog No.: ab154058, Abcam), IL-4 (1:1000, Catalog No.: ab9811, Abcam), IL-10 (1:1000, Catalog No.: ab189392, Abcam), GATA3 (1:1000, Catalog No.: ab182747, Abcam), GAPDH (1: 10000, Catalog No.: ab181603, Abcam). On the next day, the products were incubated by horseradish peroxidase (HRP)-labeled secondary antibody (goat anti-rabbit, 1: 10000, Catalog No.: ab97080, Abcam, USA) at room temperature for 1 h. Finally, development was accomplished with aid of Immobilon™ Western Chemiluminescent kit (Merck Millipore, USA), and proteins were quantified utilizing image-pro plus 5.0 software.

Quantitative real-time polymerase chain reaction (qRT-PCR)

Total RNAs were extracted from tissues, cells and blood samples utilizing RNAiso Plus reagent (TakaRa, Japan), and integrity of the RNAs was confirmed by agarose gel electrophoresis. The RNAs were reversely transcribed into cDNAs on the strength of SYBR green-based qRT-PCR kit (Invitrogen, USA). With primers (Table 1 and Supplementary Table 5) designed and synthesized by Genepharma (China), cDNAs were amplified by PCR under conditions of: 1) 95º C for 10 min, and 2) 40 cycles of 95° C for 15 s and 60º C for 1 min. Relative expressions of genes were calculated in accordance with $2^{-\Delta\Delta Ct}$ method.

Dual-luciferase reporter gene assay

PVT1 fragments that incorporated binding sites with miR-15a-5p/miR-140-5p/miR-20b-5p/miR-488-3p/miR-

Table 1. The sequences of the primers for the amplification used by real-time PCR.

Subject	Primers (5'-3')	
	Forward	Reverse
GATA3	CGAGAAAGAGTGCCTCAAGTACC	GAAGTCCTCCAGTGAGTCATGC
T-bet	GTGACCCAGATGATTGTGCT	GGTTGGGTAGGAGAGGAGAG
β-actin	TGGGTCAGAAGGATTCCTAT	ATGAGGTAGTCAGTCAGGTCC
PVT1	TGAGAACTGTCCTTACGTGACC	AGAGCACCAAGACTGGCTCT
GAPDH	CGTGTTCCTACCCCCAATGT	TGTCATACTTGGCAGGTTTCT
miR-15a-5p	ATCCAGTGCGTGTCGTG	TGCTTAGCAGCACATAATG
miR-29c-3p	GCCTAGCACCATTTGAAATCG	GTGCAGGGTCCGAGGT
U6	CTCGCTTCGGCAGCACA	ACGCTTCACGAATTTGCGT

455-5p were, respectively, amplified by PCR, so that PVT1-wide type (Wt) fragments corresponding to each miRNA were produced. On the other hand, PVT1-mutant type (Mut) fragments were generated similarly, except that binding sites with miR-15a-5p/miR-140-5p/miR-20b-5p/miR-488-3p/miR-455-5p were mutated in PVT1 fragments. Then PVT1 fragments were inserted into pGL3-Promoter plasmid vector (Promega, USA), so that pGL3-PVT1-Wt and pGL3-PVT1-Mut for each miRNA were constructed. Subsequently, miR-15a-5p mimic/miR-140-5p mimic/miR-20b-5p mimic/miR-488-3p mimic/miR-455-5p mimic/miR-NC (Genepharma, China) were co-transfected with pGL3-PVT1-Wt, pGL3-PVT1-Mut or pRL-TK plasmid (Promega, USA) into CD^{4+} T cells, and miR-29c-3p mimic/miR-143-3p mimic/miR-511-3p mimic/miR-497-5p mimic/miR-488-3p mimic/miR-NC (Genepharma, China) were co-transfected with pGL3-PVT1-Wt, pGL3-PVT1-Mut or pRL-TK plasmid into ASMCs. After 12-h incubation in 5% CO_2 at 37° C, firefly luciferase activity and renin luciferase activity of CD^{4+} T cells and ASMCs were monitored on the microplate reader (BioTek, USA), in accordance with instructions of dual luciferase reporter gene detection kit (Promega, USA).

Statistical analyses

All the data were statistically analyzed by SPSS19.0 software. Quantitative data, presented as mean ± standard deviation, were compared with student's t test or one-way analysis of variance (ANOVA). Interaction of ozone and OVA on airway smooth muscle function and Th1/Th2 cytokine level were appraised by 2×2 factorial design, and correlation matrix was established utilizing "ggcorrplot" package of R studio software (http://www.rproject.org). It was statistically significant if *P* was smaller than 0.05.

Ethics approval

All these operations and experimental process have been approved by the experimental animal ethics committee of The First Hospital of Shanxi Medical University.

Abbreviations

OVA: ovalbumin; ASMCs: airway smooth muscle cells; MCH: methacholine; AHR: airway hyper-responsiveness; HA: hyaluronan; HE: hematoxylin-eosin; PI: propidium iodide; PVDF: polyvinylidene fluoride; SDS-PAGE: sodium dodecyl sulfate-polyacrylamide gel electrophoresis; HRP: horseradish peroxidase.

AUTHOR CONTRIBUTIONS

Yangyang Wei, Baofen Han, Wenjuan Dai, Shufang Guo, Caiping Zhang, Lixuan Zhao, Yan Gao, Yi Jiang, Xiaomei Kong: conceived and designed the experiments. Yangyang Wei, Baofen Han, Wenjuan Dai, Shufang Guo: performed the experiments. Caiping Zhang, Lixuan Zhao: analyzed the data. Yan Gao, Yi Jiang, Xiaomei Kong: drafted the manuscript. All authors read and approved the final manuscript.

CONFLICTS OF INTEREST

The authors declare that they have no conflicts of interest.

FUNDING

This study was supported by the Key Research and Development Project of Shanxi Province (201903D421072).

REFERENCES

1. Reddel HK, Bateman ED, Becker A, Boulet LP, Cruz AA, Drazen JM, Haahtela T, Hurd SS, Inoue H, de Jongste JC, Lemanske RF Jr, Levy ML, O'Byrne PM, et al. A summary of the new GINA strategy: a roadmap to asthma control. Eur Respir J. 2015; 46:622–39. https://doi.org/10.1183/13993003.00853-2015 PMID:26206872

2. Rabe KF. Update in asthma 2015. Am J Respir Crit Care Med. 2016; 194:259–64. https://doi.org/10.1164/rccm.201602-0222UP PMID:27479060

3. Masoli M, Fabian D, Holt S, Beasley R, and Global Initiative for Asthma (GINA) Program. The global burden of asthma: executive summary of the GINA dissemination committee report. Allergy. 2004; 59:469–78. https://doi.org/10.1111/j.1398-9995.2004.00526.x PMID:15080825

4. O'Reilly R, Ullmann N, Irving S, Bossley CJ, Sonnappa S, Zhu J, Oates T, Banya W, Jeffery PK, Bush A, Saglani S. Increased airway smooth muscle in preschool wheezers who have asthma at school age. J Allergy Clin Immunol. 2013; 131:1024–32. https://doi.org/10.1016/j.jaci.2012.08.044 PMID:23069488

5. Baldwin L, Roche WR. Does remodelling of the airway wall precede asthma? Paediatr Respir Rev. 2002; 3:315–20. https://doi.org/10.1016/s1526054202002610 PMID:12457602

6. Chung KF, Wenzel SE, Brozek JL, Bush A, Castro M, Sterk PJ, Adcock IM, Bateman ED, Bel EH, Bleecker ER, Boulet LP, Brightling C, Chanez P, et al. International ERS/ATS guidelines on definition, evaluation and treatment of severe asthma. Eur Respir J. 2014; 43:343–73. https://doi.org/10.1183/09031936.00202013 PMID:24337046

7. Olin JT, Wechsler ME. Asthma: pathogenesis and novel drugs for treatment. BMJ. 2014; 349:g5517. https://doi.org/10.1136/bmj.g5517 PMID:25420994

8. Svensson Holm AC, Bengtsson T, Grenegård M, Lindström EG. Platelets stimulate airway smooth muscle cell proliferation through mechanisms involving 5-lipoxygenase and reactive oxygen species. Platelets. 2008; 19:528–36. https://doi.org/10.1080/09537100802320300 PMID:18979365

9. Doeing DC, Solway J. Airway smooth muscle in the pathophysiology and treatment of asthma. J Appl Physiol (1985). 2013; 114:834–43. https://doi.org/10.1152/japplphysiol.00950.2012 PMID:23305987

10. Wu Q, Tang Y, Hu X, Wang Q, Lei W, Zhou L, Huang J. Regulation of Th1/Th2 balance through OX40/OX40L signalling by glycyrrhizic acid in a murine model of asthma. Respirology. 2016; 21:102–11. https://doi.org/10.1111/resp.12655 PMID:26467500

11. Yang C, Wu D, Gao L, Liu X, Jin Y, Wang D, Wang T, Li X. Competing endogenous RNA networks in human cancer: hypothesis, validation, and perspectives. Oncotarget. 2016; 7:13479–90. https://doi.org/10.18632/oncotarget.7266 PMID:26872371

12. Zech A, Ayata CK, Pankratz F, Meyer A, Baudiß K, Cicko S, Yegutkin GG, Grundmann S, Idzko M. MicroRNA-155 modulates P2R signaling and Th2 priming of dendritic cells during allergic airway inflammation in mice. Allergy. 2015; 70:1121–29. https://doi.org/10.1111/all.12643 PMID:25944053

13. Liang Z, Tang F. The potency of lncRNA MALAT1/miR-155/CTLA4 axis in altering Th1/Th2 balance of asthma. Biosci Rep. 2020; 40:BSR20190397. https://doi.org/10.1042/BSR20190397 PMID:31909418

14. Perry MM, Tsitsiou E, Austin PJ, Lindsay MA, Gibeon DS, Adcock IM, Chung KF. Role of non-coding RNAs in maintaining primary airway smooth muscle cells. Respir Res. 2014; 15:58. https://doi.org/10.1186/1465-9921-15-58 PMID:24886442

15. Austin PJ, Tsitsiou E, Boardman C, Jones SW, Lindsay MA, Adcock IM, Chung KF, Perry MM. Transcriptional profiling identifies the long noncoding RNA plasmacytoma variant translocation (PVT1) as a novel regulator of the asthmatic phenotype in human airway smooth muscle. J Allergy Clin Immunol. 2017; 139:780–89. https://doi.org/10.1016/j.jaci.2016.06.014 PMID:27484035

16. Schatz M, Rosenwasser L. The allergic asthma phenotype. J Allergy Clin Immunol Pract. 2014; 2:645–48. https://doi.org/10.1016/j.jaip.2014.09.004 PMID:25439351

17. Pribilla W. [Blood and blood diseases]. Munch Med Wochenschr. 1961; 103:2001–05. PMID:14488722

18. McConnell R, Berhane K, Gilliland F, London SJ, Islam T, Gauderman WJ, Avol E, Margolis HG, Peters JM. Asthma in exercising children exposed to ozone: a cohort study. Lancet. 2002; 359:386–91. https://doi.org/10.1016/S0140-6736(02)07597-9 PMID:11844508

19. Moore BD, Hyde D, Miller L, Wong E, Frelinger J, Schelegle ES. Allergen and ozone exacerbate serotonin-induced increases in airway smooth muscle contraction in a model of childhood asthma. Respiration. 2012; 83:529–42. https://doi.org/10.1159/000336835 PMID:22507883

20. Seltzer J, Bigby BG, Stulbarg M, Holtzman MJ, Nadel JA, Ueki IF, Leikauf GD, Goetzl EJ, Boushey HA. O3-induced change in bronchial reactivity to methacholine and airway inflammation in humans. J Appl Physiol (1985). 1986; 60:1321–26. https://doi.org/10.1152/jappl.1986.60.4.1321 PMID:3084448

21. Wu D, Tan W, Zhang Q, Zhang X, Song H. Effects of ozone exposure mediated by BEAS-2B cells on T cells activation: a possible link between environment and asthma. Asian Pac J Allergy Immunol. 2014; 32:25–33. PMID:24641287

22. Fuentes N, Roy A, Mishra V, Cabello N, Silveyra P. Sex-specific microRNA expression networks in an acute mouse model of ozone-induced lung inflammation. Biol Sex Differ. 2018; 9:18. https://doi.org/10.1186/s13293-018-0177-7 PMID:29739446

23. Chen QZ, Zhou YB, Zhou LF, Fu ZD, Wu YS, Chen Y, Li SN, Huang JR, Li JH. TRPC6 modulates adhesion of neutrophils to airway epithelial cells via NF-κB activation and ICAM-1 expression with ozone exposure. Exp Cell Res. 2019; 377:56–66. https://doi.org/10.1016/j.yexcr.2019.02.013 PMID:30779919

24. Clay CC, Maniar-Hew K, Gerriets JE, Wang TT, Postlethwait EM, Evans MJ, Fontaine JH, Miller LA. Early life ozone exposure results in dysregulated innate immune function and altered microRNA expression in airway epithelium. PLoS One. 2014; 9:e90401. https://doi.org/10.1371/journal.pone.0090401 PMID:24594710

25. Li JH, Liu S, Zhou H, Qu LH, Yang JH. starBase v2.0: decoding miRNA-ceRNA, miRNA-ncRNA and protein-RNA interaction networks from large-scale CLIP-seq data. Nucleic Acids Res. 2014; 42:D92–97. https://doi.org/10.1093/nar/gkt1248 PMID:24297251

26. Vlachos IS, Kostoulas N, Vergoulis T, Georgakilas G, Reczko M, Maragkakis M, Paraskevopoulou MD, Prionidis K, Dalamagas T, Hatzigeorgiou AG. DIANA miRPath v.2.0: investigating the combinatorial effect of microRNAs in pathways. Nucleic Acids Res. 2012; 40:W498–504. https://doi.org/10.1093/nar/gks494 PMID:22649059

27. Lin HY, Xu L, Xie SS, Yu F, Hu HY, Song XL, Wang CH. Mesenchymal stem cells suppress lung inflammation and airway remodeling in chronic asthma rat model via PI3K/Akt signaling pathway. Int J Clin Exp Pathol. 2015; 8:8958–67. PMID:26464637

28. Wang J, Li F, Yang M, Wu J, Zhao J, Gong W, Liu W, Bi W, Dong L. FIZZ1 promotes airway remodeling through the PI3K/Akt signaling pathway in asthma. Exp Ther Med. 2014; 7:1265–70. https://doi.org/10.3892/etm.2014.1580 PMID:24940423

29. Sinclair C, Bommakanti G, Gardinassi L, Loebbermann J, Johnson MJ, Hakimpour P, Hagan T, Benitez L, Todor A, Machiah D, Oriss T, Ray A, Bosinger S, et al. mTOR regulates metabolic adaptation of APCs in the lung and controls the outcome of allergic inflammation. Science. 2017; 357:1014–21. https://doi.org/10.1126/science.aaj2155 PMID:28798047

30. Zhang Y, Jing Y, Qiao J, Luan B, Wang X, Wang L, Song Z. Activation of the mTOR signaling pathway is required for asthma onset. Sci Rep. 2017; 7:4532. https://doi.org/10.1038/s41598-017-04826-y PMID:28674387

31. Shao Y, Chong L, Lin P, Li H, Zhu L, Wu Q, Li C. MicroRNA-133a alleviates airway remodeling in asthtama through PI3K/AKT/mTOR signaling pathway by targeting IGF1R. J Cell Physiol. 2019; 234:4068–80. https://doi.org/10.1002/jcp.27201 PMID:30146725

32. Kramer EL, Hardie WD, Mushaben EM, Acciani TH, Pastura PA, Korfhagen TR, Hershey GK, Whitsett JA, Le Cras TD. Rapamycin decreases airway remodeling and hyperreactivity in a transgenic model of noninflammatory lung disease. J Appl Physiol (1985). 2011; 111:1760–67. https://doi.org/10.1152/japplphysiol.00737.2011 PMID:21903885

33. Xiao W, Tang H, Wu M, Liao Y, Li K, Li L, Xu X. Ozone oil promotes wound healing by increasing the migration of fibroblasts via PI3K/Akt/mTOR signaling pathway. Biosci Rep. 2017; 37:BSR20170658. https://doi.org/10.1042/BSR20170658 PMID:28864782

34. Umoh NA, Walker RK, Al-Rubaiee M, Jeffress MA, Haddad GE. Acute alcohol modulates cardiac function as PI3K/Akt regulates oxidative stress. Alcohol Clin Exp Res. 2014; 38:1847–64. https://doi.org/10.1111/acer.12459 PMID:24962888

35. Kumar RK, Foster PS. Modeling allergic asthma in mice: pitfalls and opportunities. Am J Respir Cell Mol Biol. 2002; 27:267–72. https://doi.org/10.1165/rcmb.F248 PMID:12204888

36. Matsubara S, Takeda K, Jin N, Okamoto M, Matsuda H, Shiraishi Y, Park JW, McConville G, Joetham A, O'Brien RL, Dakhama A, Born WK, Gelfand EW. Vgamma1+ T cells and tumor necrosis factor-alpha in ozone-induced

airway hyperresponsiveness. Am J Respir Cell Mol Biol. 2009; 40:454–63.
https://doi.org/10.1165/rcmb.2008-0346OC
PMID:18927346

37. Hamelmann E, Schwarze J, Takeda K, Oshiba A, Larsen GL, Irvin CG, Gelfand EW. Noninvasive measurement of airway responsiveness in allergic mice using barometric plethysmography. Am J Respir Crit Care Med. 1997; 156:766–75.
https://doi.org/10.1164/ajrccm.156.3.9606031
PMID:9309991

38. Knobloch J, Yanik SD, Körber S, Stoelben E, Jungck D, Koch A. TNFα-induced airway smooth muscle cell proliferation depends on endothelin receptor signaling, GM-CSF and IL-6. Biochem Pharmacol. 2016; 116:188–99.
https://doi.org/10.1016/j.bcp.2016.07.008
PMID:27422754

39. Kothapalli D, Zhao L, Hawthorne EA, Cheng Y, Lee E, Puré E, Assoian RK. Hyaluronan and CD44 antagonize mitogen-dependent cyclin D1 expression in mesenchymal cells. J Cell Biol. 2007; 176:535–44.
https://doi.org/10.1083/jcb.200611058
PMID:17296798

40. Kothapalli D, Flowers J, Xu T, Puré E, Assoian RK. Differential activation of ERK and rac mediates the proliferative and anti-proliferative effects of hyaluronan and CD44. J Biol Chem. 2008; 283:31823–29.
https://doi.org/10.1074/jbc.M802934200
PMID:18806267

41. Jain M, He Q, Lee WS, Kashiki S, Foster LC, Tsai JC, Lee ME, Haber E. Role of CD44 in the reaction of vascular smooth muscle cells to arterial wall injury. J Clin Invest. 1996; 98:877.
PMID:8698880

42. Shirakawa T, Enomoto T, Shimazu S, Hopkin JM. The inverse association between tuberculin responses and atopic disorder. Science. 1997; 275:77–79.
https://doi.org/10.1126/science.275.5296.77
PMID:8974396

43. Rengarajan J, Szabo SJ, Glimcher LH. Transcriptional regulation of Th1/Th2 polarization. Immunol Today. 2000; 21:479–83.
https://doi.org/10.1016/s0167-5699(00)01712-6
PMID:11071525

44. Garantziotis S, Li Z, Potts EN, Kimata K, Zhuo L, Morgan DL, Savani RC, Noble PW, Foster WM, Schwartz DA, Hollingsworth JW. Hyaluronan mediates ozone-induced airway hyperresponsiveness in mice. J Biol Chem. 2009; 284:11309–17.
https://doi.org/10.1074/jbc.M802400200
PMID:19164299

45. Williams AS, Issa R, Durham A, Leung SY, Kapoun A, Medicherla S, Higgins LS, Adcock IM, Chung KF. Role of p38 mitogen-activated protein kinase in ozone-induced airway hyperresponsiveness and inflammation. Eur J Pharmacol. 2008; 600:117–22.
https://doi.org/10.1016/j.ejphar.2008.09.031
PMID:18926814

46. Williams AS, Leung SY, Nath P, Khorasani NM, Bhavsar P, Issa R, Mitchell JA, Adcock IM, Chung KF. Role of TLR2, TLR4, and MyD88 in murine ozone-induced airway hyperresponsiveness and neutrophilia. J Appl Physiol (1985). 2007; 103:1189–95.
https://doi.org/10.1152/japplphysiol.00172.2007
PMID:17626835

47. Vagaggini B, Bartoli ML, Cianchetti S, Costa F, Bacci E, Dente FL, Di Franco A, Malagrinò L, Paggiaro P. Increase in markers of airway inflammation after ozone exposure can be observed also in stable treated asthmatics with minimal functional response to ozone. Respir Res. 2010; 11:5.
https://doi.org/10.1186/1465-9921-11-5
PMID:20085630

48. Bosson J, Stenfors N, Bucht A, Helleday R, Pourazar J, Holgate ST, Kelly FJ, Sandström T, Wilson S, Frew AJ, Blomberg A. Ozone-induced bronchial epithelial cytokine expression differs between healthy and asthmatic subjects. Clin Exp Allergy. 2003; 33:777–82.
https://doi.org/10.1046/j.1365-2222.2003.01662.x
PMID:12801312

49. Basha MA, Gross KB, Gwizdala CJ, Haidar AH, Popovich J Jr. Bronchoalveolar lavage neutrophilia in asthmatic and healthy volunteers after controlled exposure to ozone and filtered purified air. Chest. 1994; 106:1757–65.
https://doi.org/10.1378/chest.106.6.1757
PMID:7988196

50. Ochs-Balcom HM, Grant BJ, Muti P, Sempos CT, Freudenheim JL, Browne RW, McCann SE, Trevisan M, Cassano PA, Iacoviello L, Schünemann HJ. Antioxidants, oxidative stress, and pulmonary function in individuals diagnosed with asthma or COPD. Eur J Clin Nutr. 2006; 60:991–99.
https://doi.org/10.1038/sj.ejcn.1602410
PMID:16482071

51. Cheng YK, Tsai MH, Lin CD, Hwang GY, Hang LW, Tseng GC, Shen PS, Chang WC. Oxidative stress in nonallergic nasal polyps associated with bronchial hyperresponsiveness. Allergy. 2006; 61:1290–98.
https://doi.org/10.1111/j.1398-9995.2006.01228.x
PMID:17002704

52. To T, Stanojevic S, Moores G, Gershon AS, Bateman ED, Cruz AA, Boulet LP. Global asthma prevalence in adults:

findings from the cross-sectional world health survey. BMC Public Health. 2012; 12:204. https://doi.org/10.1186/1471-2458-12-204 PMID:22429515

53. Jia L, Landan G, Pomerantz M, Jaschek R, Herman P, Reich D, Yan C, Khalid O, Kantoff P, Oh W, Manak JR, Berman BP, Henderson BE, et al. Functional enhancers at the gene-poor 8q24 cancer-linked locus. PLoS Genet. 2009; 5:e1000597. https://doi.org/10.1371/journal.pgen.1000597 PMID:19680443

54. Li T, Meng XL, Yang WQ. Long noncoding RNA PVT1 acts as a "sponge" to inhibit microRNA-152 in gastric cancer cells. Dig Dis Sci. 2017; 62:3021–28. https://doi.org/10.1007/s10620-017-4508-z PMID:28258379

55. Nakano T, Inoue Y, Shimojo N, Yamaide F, Morita Y, Arima T, Tomiita M, Kohno Y. Lower levels of hsa-mir-15a, which decreases VEGFA, in the CD4+ T cells of pediatric patients with asthma. J Allergy Clin Immunol. 2013; 132:1224–27.e12. https://doi.org/10.1016/j.jaci.2013.06.041 PMID:23954351

56. Liu X, Wang L, Li H, Lu X, Hu Y, Yang X, Huang C, Gu D. Coactivator-associated arginine methyltransferase 1 targeted by miR-15a regulates inflammation in acute coronary syndrome. Atherosclerosis. 2014; 233:349–56. https://doi.org/10.1016/j.atherosclerosis.2014.01.039 PMID:24530761

57. He Z, Liao Z, Chen S, Li B, Yu Z, Luo G, Yang L, Zeng C, Li Y. Downregulated miR-17, miR-29c, miR-92a and miR-214 may be related to BCL11B overexpression in T cell acute lymphoblastic leukemia. Asia Pac J Clin Oncol. 2018; 14:e259–65. https://doi.org/10.1111/ajco.12979 PMID:29749698

58. Zhang X, Zhao X, Sun H, Yan Y, Huang L, Gu W, Jiang W, Wang Y, Zhu C, Ji W, Hao C, Chen Z. The role of miR-29c/B7-H3 axis in children with allergic asthma. J Transl Med. 2018; 16:218. https://doi.org/10.1186/s12967-018-1590-8 PMID:30075787

59. Yoo JK, Kim J, Choi SJ, Noh HM, Kwon YD, Yoo H, Yi HS, Chung HM, Kim JK. Discovery and characterization of novel microRNAs during endothelial differentiation of human embryonic stem cells. Stem Cells Dev. 2012; 21:2049–57. https://doi.org/10.1089/scd.2011.0500 PMID:22142236

60. Bang C, Fiedler J, Thum T. Cardiovascular importance of the microRNA-23/27/24 family. Microcirculation. 2012; 19:208–14. https://doi.org/10.1111/j.1549-8719.2011.00153.x PMID:22136461

61. Jakob P, Landmesser U. Role of microRNAs in stem/progenitor cells and cardiovascular repair. Cardiovasc Res. 2012; 93:614–22. https://doi.org/10.1093/cvr/cvr311 PMID:22135162

62. Liu F, Lou YL, Wu J, Ruan QF, Xie A, Guo F, Cui SP, Deng ZF, Wang Y. Upregulation of microRNA-210 regulates renal angiogenesis mediated by activation of VEGF signaling pathway under ischemia/perfusion injury in vivo and in vitro. Kidney Blood Press Res. 2012; 35:182–91. https://doi.org/10.1159/000331054 PMID:22123256

63. Mun J, Tam C, Chan G, Kim JH, Evans D, Fleiszig S. MicroRNA-762 is upregulated in human corneal epithelial cells in response to tear fluid and pseudomonas aeruginosa antigens and negatively regulates the expression of host defense genes encoding RNase7 and ST2. PLoS One. 2013; 8:e57850. https://doi.org/10.1371/journal.pone.0057850 PMID:23469087

64. Condliffe AM, Cadwallader KA, Walker TR, Rintoul RC, Cowburn AS, Chilvers ER. Phosphoinositide 3-kinase: a critical signalling event in pulmonary cells. Respir Res. 2000; 1:24–29. https://doi.org/10.1186/rr8 PMID:11667961

65. Ward SG, Finan P. Isoform-specific phosphoinositide 3-kinase inhibitors as therapeutic agents. Curr Opin Pharmacol. 2003; 3:426–34. https://doi.org/10.1016/s1471-4892(03)00078-x PMID:12901953

66. Arimura Y, Shiroki F, Kuwahara S, Kato H, Dianzani U, Uchiyama T, Yagi J. Akt is a neutral amplifier for th cell differentiation. J Biol Chem. 2004; 279:11408–16. https://doi.org/10.1074/jbc.M309063200 PMID:14707136

67. Scott PH, Belham CM, al-Hafidh J, Chilvers ER, Peacock AJ, Gould GW, Plevin R. A regulatory role for cAMP in phosphatidylinositol 3-kinase/p70 ribosomal S6 kinase-mediated DNA synthesis in platelet-derived-growth-factor-stimulated bovine airway smooth-muscle cells. Biochem J. 1996; 318:965–71. https://doi.org/10.1042/bj3180965 PMID:8836145

68. Follo MY, Manzoli L, Poli A, McCubrey JA, Cocco L. PLC and PI3K/Akt/mTOR signalling in disease and cancer. Adv Biol Regul. 2015; 57:10–16. https://doi.org/10.1016/j.jbior.2014.10.004 PMID:25482988

69. Yu Q, Chen X, Fang X, Chen Q, Hu C. Caveolin-1 aggravates cigarette smoke extract-induced MUC5AC secretion in human airway epithelial cells. Int J Mol Med. 2015; 35:1435–42.

https://doi.org/10.3892/ijmm.2015.2133
PMID:25776934

70. Aubier M, Thabut G, Hamidi F, Guillou N, Brard J, Dombret MC, Borensztajn K, Aitilalne B, Poirier I, Roland-Nicaise P, Taillé C, Pretolani M. Airway smooth muscle enlargement is associated with protease-activated receptor 2/ligand overexpression in patients with difficult-to-control severe asthma. J Allergy Clin Immunol. 2016; 138:729–39.e11. https://doi.org/10.1016/j.jaci.2015.12.1332 PMID:27001157

71. Dragon S, Hirst SJ, Lee TH, Gounni AS. IL-17A mediates a selective gene expression profile in asthmatic human airway smooth muscle cells. Am J Respir Cell Mol Biol. 2014; 50:1053–63. https://doi.org/10.1165/rcmb.2012-0267OC PMID:24393021

72. Abdelfattah NS, Amgad M, Zayed AA, Hussein H, Abd El-Baky N. Molecular underpinnings of corneal angiogenesis: advances over the past decade. Int J Ophthalmol. 2016; 9:768–79. https://doi.org/10.18240/ijo.2016.05.24 PMID:27275438

73. Weisel CP, Cody RP, Lioy PJ. Relationship between summertime ambient ozone levels and emergency department visits for asthma in central new jersey. Environ Health Perspect. 1995 (Suppl 2); 103:97–102. https://doi.org/10.1289/ehp.95103s297 PMID:7614954

74. Palecek F, Palecekova M, Aviado DM. Emphysema in immature rats. Condition produced by tracheal constriction and papain. Arch Environ Health. 1967; 15:332–42. https://doi.org/10.1080/00039896.1967.10664929 PMID:6035083

75. Association RBoCM. Guidelines for Prevention and Treatment of Bronchial Asthma. Chinese Journal of Tuberculosis and Respiratory Diseases. 1997; 20:261–7.

SUPPLEMENTARY MATERIALS

Supplementary Figures

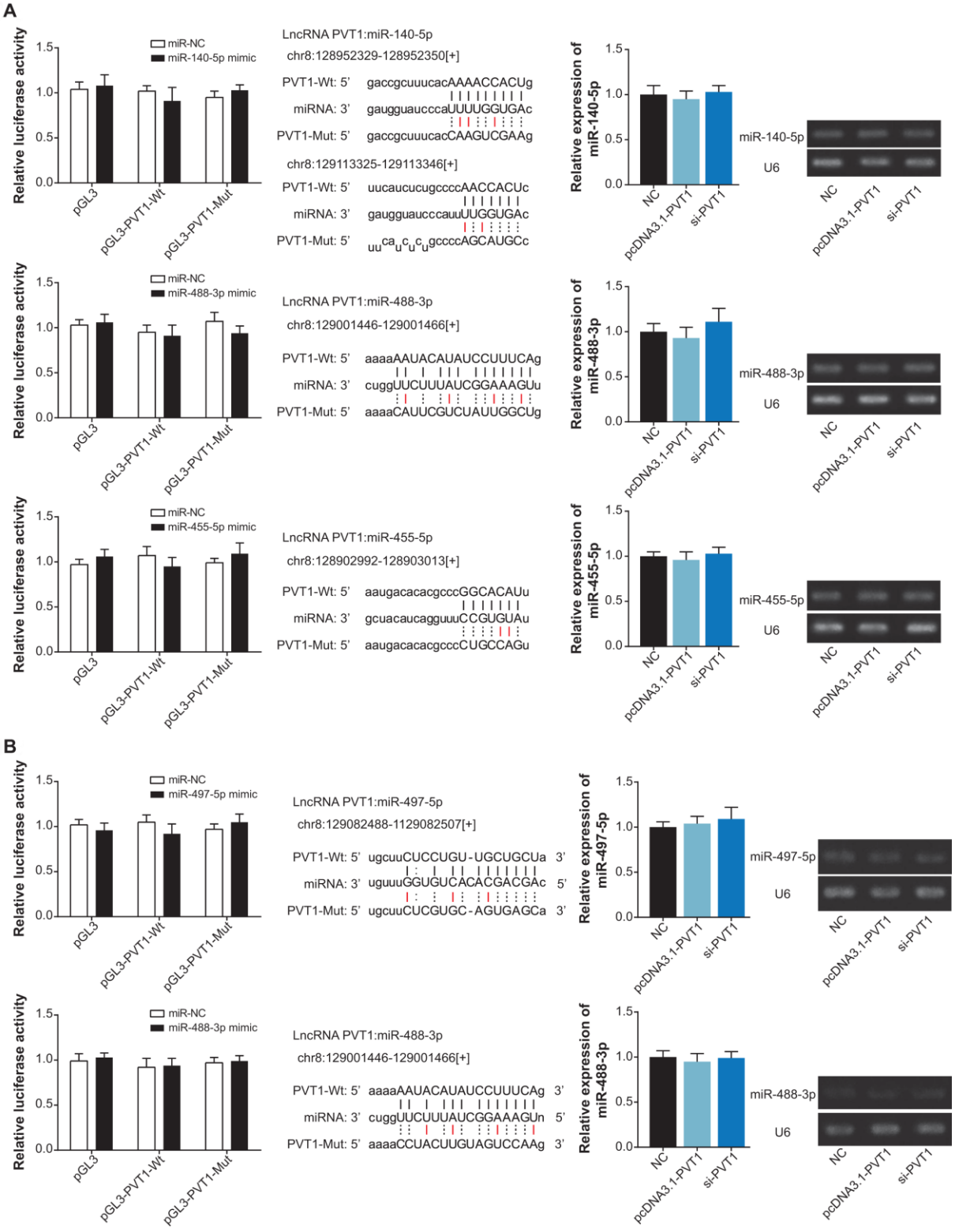

Supplementary Figure 1. MiRNAs failed to be sponged by lncRNA PVT1 within CD^{4+} T cells (**A**) and ASMCs (**B**).

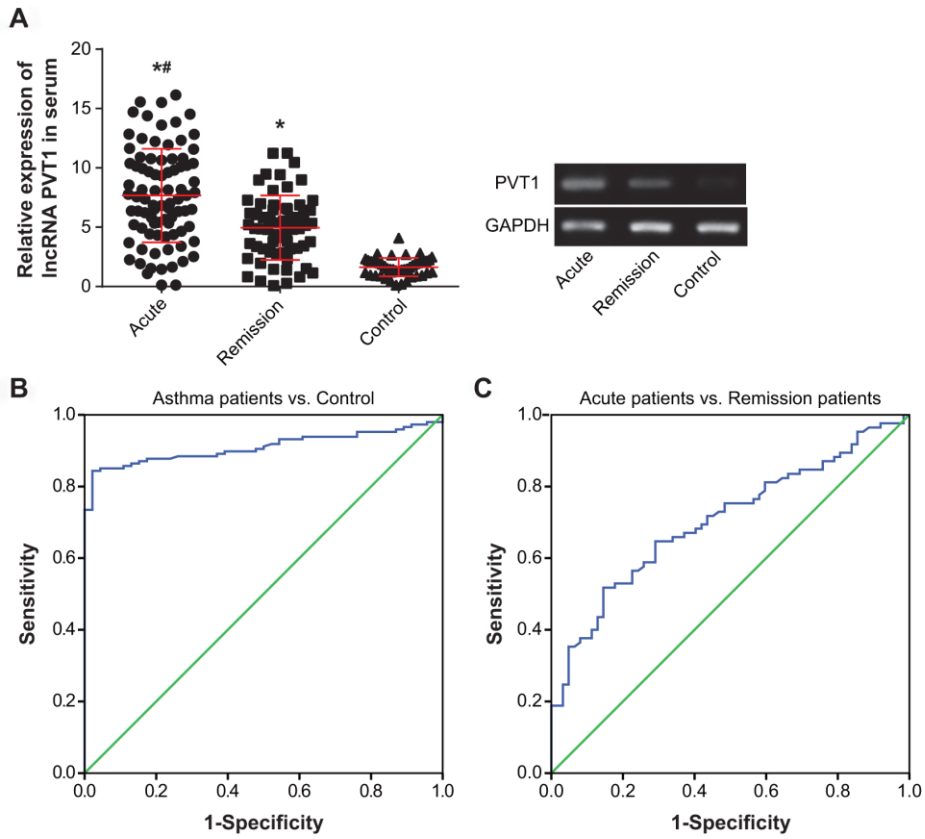

Supplementary Figure 2. Diagnostic performance of lncRNA PVT1 for asthma. (**A**) Serum level of lncRNA PVT1 was determined among patients at the acute stage of asthma, asthma patients in remission stage and healthy volunteers. (**B**) ROC curve was plotted to estimate the role of lncRNA PVT1 in diagnosis of asthma. (**C**) Serum level of lncRNA PVT1 was powerful in separating patients at the acute stage of asthma from asthma patients in remission stage.

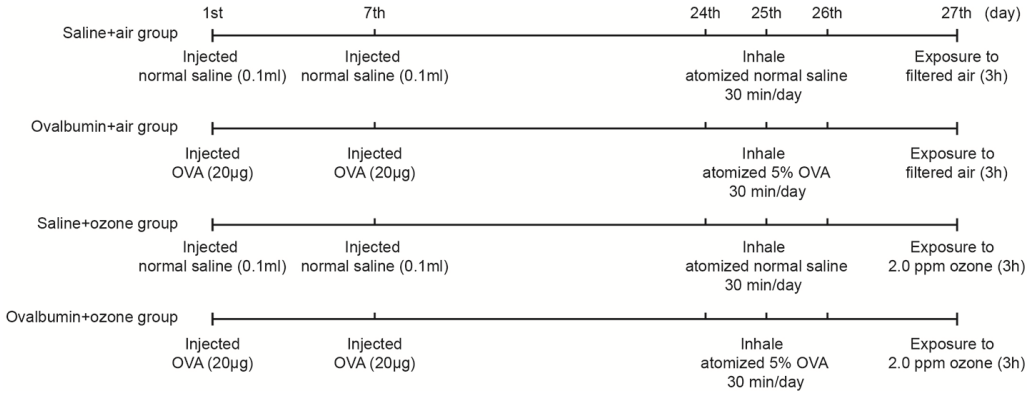

Supplementary Figure 3. The treatment scheme for establishing mice models. 1) mice in the saline+air group (control group) were intraperitoneally injected with 0.1 ml normal saline that contained 2 mg white alum on the 1st day and 7th day, and then they were scheduled to inhale atomized normal saline for 30 min on the 24th day, 25th day and 26th day, and to exposure to filtered air for 3 h on the 27th day; 2) mice in the OVA+air group (asthma group) were treated in much the same way as those in the control group, except that they were injected with 20 μg OVA (grade V, Sigma-Aldrich, USA), rather than white alum, on the 1st day and 7th day, and they and they inhaled atomized 5% OVA, instead of normal saline, on the 24th, 25th and 26th days; 3) mice in the saline+ozone group were also treated in an approach most identically to the control group, except that they were exposed to 2.0 ppm ozone, rather than filtered air, on the 27th day; and 4) mice in the OVA+ozone group were treated in a way much the same as asthma group, except that mice were exposed to 2.0 ppm ozone, rather than filtered air, on the 27th day.

Supplementary Tables

Supplementary Table 1. Ozone concentrations in 2016.

Country	Concentrations (ppb)	Country	Concentrations (ppb)
Afghanistan	63	Libya	61
Albania	68	Lithuania	51
Algeria	70	Luxembourg	54
Angola	88	Macedonia	66
Argentina	40	Madagascar	40
Armenia	62	Malawi	53
Australia	36	Malaysia	49
Austria	59	Mali	50
Azerbaijan	59	Mauritania	44
Bangladesh	75	Mexico	59
Belarus	51	Moldova	58
Belgium	54	Mongolia	49
Belize	46	Montenegro	64
Benin	71	Morocco	58
Bhutan	70	Mozambique	48
Bolivia	63	Myanmar	82
Bosnia and Herzegovina	64	Namibia	61
Botswana	59	Nepal	79
Brazil	54	Netherlands	53
Bulgaria	65	New Zealand	35
Burundi	53	Nicaragua	41
Cambodia	51	Niger	52
Cameroon	67	Nigeria	67
Canada	56	North Korea	70
Central African Republic	77	Norway	45
Chad	60	Oman	79
Chile	43	Pakistan	70
China	66	Palestine	72
Colombia	49	Panama	43
Congo	62	Papua New Guinea	29
Costa Rica	41	Paraguay	58
Cote d'lvoire	61	Peru	45
Croatia	65	Philippines	40
Cuba	48	Poland	55
Cyprus	68	Portugal	54
Czech Republic	58	Puerto Rico	42
Democratic Republic of Congo	64	Qatar	117
Denmark	50	Romania	59
Dominican Republic	45	Russia	48
Ecuador	42	Rwanda	52
Egypt	70	Saudi Arabia	69
El Salvador	57	Senegal	45
Equatorial Guinea	53	Serbia	61

Eritrea	47	Sierra Leone	58
Estonia	48	Slovakia	60
Ethiopia	51	Slovenia	64
Fiji	35	Solomon Islands	28
Finland	46	Somalia	40
France	56	South Africa	53
Gabon	51	South Korea	69
Georgia	59	South Sudan	64
Germany	55	Spain	61
Ghana	66	Sudan	51
Greece	69	Suriname	34
Greenland	34	Swaziland	51
Guatemala	57	Sweden	46
Guinea	60	Switzerland	59
Guyana	32	Syria	70
Haiti	47	Taiwan	70
Honduras	45	Tajikistan	64
Hungary	61	Tanzania	47
Iceland	45	Thailand	59
India	77	Timor-Leste	37
Indonesia	44	Togo	72
Iran	74	Tunisia	67
Iraq	75	Turkey	67
Ireland	48	Turkmenistan	59
Israel	71	Uganda	51
Italy	74	Ukraine	57
Jamaica	44	United Arab Emirates	103
Japan	62	United Kingdom	49
Jordan	73	United States	66
Kazakhstan	52	Uruguay	39
Kenya	42	Uzbekistan	63
Kuwait	84	Vanuatu	37
Kyrgyzstan	65	Venezuela	48
Laos	63	Vietnam	56
Latvia	49	Yemen	54
Lebanon	71	Zambia	64
Lesotho	55	Zimbabwe	58
Liberia	55		

Supplementary Table 2. Asthma diagnosis around the world.

Region	Country	Doctor Diagnosed Asthma (%)	Clinical Asthma (%)	Wheezing Symptoms (%)
Africa	Burkina Faso	2.02	2.26	5.32
	Chad	3.68	3.94	7.64
	Comoros	7.55	7.8	12.85
	Congo	4.65	4.79	7.93
	Cote d'Iviore	4.22	4.59	7.7
	Ethiopia	2	2	5.53
	Ghana	3.65	3.77	4.88
	Kenya	2.86	3.12	6.22
	Malawi	4.62	4.67	7.76
	Mali	2.65	2.82	4.77
	Mauritania	6.95	7.54	11.78
	Mauritius	3.88	3.92	6.88
	Namibia	3.16	3.39	8.14
	Senegal	3.43	3.72	8.4
	South Africa	5.92	6.09	12.4
	Swaziland	8.74	9.69	15.37
	Zambia	2.83	2.96	6.25
	Zimbabwe	2.28	2.52	5.48
Regional Sub-total		3.94	4.19	7.75
Americas	Brazil	12.44	12.98	22.56
	Dominican	9.63	9.97	12.39
	Ecuador	2.03	2.13	3.83
	Guatemala	2.26	2.42	11.95
	Mexico	2.39	2.39	3.87
	Paraguay	6.08	6.4	12.74
	Uruguay	8.6	9.1	12.02
Regional Sub-total		4.27	4.4	7.61
Eastern Mediterranean	Morocco	2.76	2.84	11.65
	Pakistan	3.12	3.13	5.02
	Tunisia	2.74	2.79	7.21
	United Arab Emirates	5.3	2.79	7.21
Regional Sub-total		2.93	2.99	7.6
Europe	Austria	7.46	7.63	9.48
	Belgium	9.83	10	17.22
	Bosnia Herzegovina	1.3	1.41	4.01
	Crotia	4.38	4.57	8.66
	Czech Republic	4.56	4.71	6.32
	Denmark	9.5	10.19	15.4
	Estonia	2	1.99	6.94
	Finland	9.39	10.24	17.19
	France	10.43	10.59	15.2
	Georgia	2.09	2.15	4.83
	Germany	7.58	7.55	9.25

	Greece	6.6	6.84	10.14
	Hungary	7.66	7.66	14.72
	Ireland	9.41	9.19	11.39
	Israel	7.59	8.54	14.98
	Italy	6.05	6.26	8.98
	Kazakhstan	1.43	1.47	3.36
	Latvia	2.7	2.7	5.9
	Luxembourg	9.16	9.44	16.63
	Netherlands	15.17	15.32	22.71
	Norway	11.05	12.32	15.05
	Portugal	7.83	7.83	8.72
	Russia	2.5	2.57	4.98
	Slovakia	4.11	4.1	7.41
	Slovenia	8.7	8.66	11.91
	Spain	6.79	7.12	12.78
	Sweden	20.09	20.18	21.6
	Turkey	2.06	2.11	11.34
	UK	17.59	18.15	22.59
	Ukraine	2.77	2.9	11.13
Regional Sub-total		5.1	5.28	10.71
South East Asia	Bangladesh	2.91	3.23	8.63
	India	3.16	3.3	9.63
	Myanmar	2.36	2.41	3.47
	Nepal	2.04	2.16	14.37
	Sri Lanka	2.6	2.75	6.35
Regional Sub-total		3.24	3.39	9.71
Western Pacific	Australia	20.96	21.51	27.39
	China	0.19	1.42	1.73
	Laos	2.72	3.02	5.16
	Malaysia	5.21	5.51	7.55
	Philippines	7.21	7.46	11.01
	Vietnam	0.82	1.04	2.05
Regional Sub-total		5.85	6.17	8.88

Supplementary Table 3. Comparison of baseline characteristics among asthma patients of acute stage, asthma patients of remission stage and healthy controls.

Clinical characteristics	Asthma acute group (N=85)	Asthma remission group (N=62)	Healthy control group (N=46)
Age (year)	38.76±10.52	40.42±8.37	41.25±9.06
Gender			
Female	40	32	21
Male	45	30	25
Disease Course (year)	5.62±3.28	6.03±4.15	-
FEV1(%)	55.26±7.68*#	81.52±9.18*	90.91±6.99
FEV1/FVC(%)	64.50±8.15*#	75.55±6.71*	86.16±10.11
TNF-α (ng/L)	2.81±0.29*#	1.41±0.27*	0.33±0.16
IL-13 (ng/L)	35.68±6.82*#	24.01±4.38*	8.42±3.06
IL-4 (ng/L)	115.37±38.26*#	55.24±17.54*	41.93±13.16
IL-10 (ng/L)	96.43±19.57*#	49.31±13.08*	36.73±9.31
IFN-γ (ng/L)	33.89±6.87*#	54.62±8.42*	69.31±9.59
IL-2 (ng/L)	118.64±38.14*#	186.32±43.13*	207.45±50.12
hs-CRP (mg/L)	13.18±3.25*#	5.22±1.03*	1.47±0.40
FeNO (ppb)	92.47±28.14*#	42.39±17.12*	14.84±4.25

* $p<0.05$ when compared with healthy control group; # $p<0.05$ when compared with asthma remission group.

Supplementary Table 4. Diagnostic efficiency of lncRNA PVT1 for asthma.

Group	Value	Sensitivity	Specificity	AUC	95% CI
Asthma vs. Group	2.83	0.844	0.978	0.909	0.87-0.95
Acute vs. Remission	7.32	0.518	0.855	0.705	0.62-0.79

Supplementary Table 5. The sequences of the primers for the amplification used by real-time PCR.

microRNA	Primers (5'-3')	
	Forward	Reverse
hsa-miR-15a-5p	ATCCAGTGCGTGTCGTG	TGCTTAGCAGCACATAATG
hsa-miR-140-5p	CCCCCAGTGGTTTTACCCTA	GTGCGTGTCGTGGAGTCG
hsa-miR-20b-5p	TGTCAACGATACGCTACGA	GCTCATAGTGCAGGTAGA
hsa-miR-488-3p	CGGGGCAGCUCAGUACAG	CAGTGCGTGTCGTGGAGT
has-miR-455-5p	CGAGCTTCCTTCTGCAGGT	CACCACTGCCATCCCACA
hsa-miR-29c-3p	GCCTAGCACCATTTGAAATCG	GTGCAGGGTCCGAGGT
hsa-miR-143-3p	GGGGTGAGATGAAGCACTG	CAGTGCGTGTCGTGGAGT
hsa-miR-511-3p	GTCTTTTGCTCTGCAGTC	GAACATGTCTGCGTATCTC
hsa-miR-497-5p	CCTTCAGCAGCACACTGTGG	CAGTGCAGGGTCCGAGGTAT

Supplementary Material

Please browse Full Text version to see the data of Supplementary Material 1.

Supplementary Material 1. MiRNAs potentially sponged by PVT1 were predicted with usage of starBase software.